

Volatility Parametrizations with Random Coefficients: Analytic Flexibility for Implied Volatility Surfaces

NICOLA F. ZAUGG^{a,c,*}, LEONARDO PEROTTI^a, LECH A. GRZELAK^{a,b}

^a*Mathematical Institute, Utrecht University, Utrecht, the Netherlands*

^b*Financial Engineering, Rabobank, Utrecht, the Netherlands*

^c*Capital Markets Technology, swissQuant Group AG, Zurich, Switzerland*

Abstract

It is a market practice to express market-implied volatilities in some parametric form. The most popular parametrizations are based on or inspired by an underlying stochastic model, like the Heston model (SVI method [9]) or the SABR model (SABR-parametrization [15]). Their popularity is often driven by a closed-form representation enabling efficient calibration. However, these representations indirectly impose a model-specific volatility structure on observable market quotes. When the market's volatility does not follow the parametric model regime, the calibration procedure will fail or lead to extreme parameters, indicating inconsistency. This article addresses this critical limitation - we propose an arbitrage-free framework for letting the parameters from the parametric implied volatility formula be random. The method enhances the existing parametrizations and enables a significant widening of the spectrum of permissible shapes of implied volatilities while preserving analyticity and, therefore, computation efficiency. We demonstrate the effectiveness of the novel method on real data from short-term index and equity options, where the standard parametrizations fail to capture market dynamics. Our results show that the proposed method is particularly powerful in modeling the implied volatility curves of short expiry options preceding an earnings announcement, when the risk-neutral probability density function exhibits a bimodal form.

Keywords: Implied Volatility Parametrizations, Randomization, Stochastic Parameters, Short-term Options, W-shaped Implied Volatility, Market-Making.

1. Introduction

Obtaining a clean implied volatility surface from the options market is a fundamental aspect of modeling financial derivatives. Volatility surfaces reflect the current price level of vanilla option contracts and are often used as inputs to advanced derivative models. The models are then utilized to price exotic derivatives, set margin requirements for derivative trades, or are used by market makers to offer the most competitive price in the options market. The essence of constructing an implied volatility surface is to encode the discrete and noisy option price quotes from the market into a clean, continuous surface, which provides a value of the Black-Scholes implied volatility for any desired combination of time to expiry and strike on a domain of interest. The main challenge is to obtain an implied volatility surface that is arbitrage-free, meaning that it does not lead to any static arbitrage opportunities for the implied option prices.

The existing literature on this problem is elaborate, and more innovative techniques are continuously being developed. This paper aims to provide a generic method to enable *implied volatility surface parametrizations* to become more effective. Inspired by the RAnD

*Corresponding author.

Email addresses: N.F.Zaugg@uu.nl (NICOLA F. ZAUGG), L.Perotti@uu.nl (LEONARDO PEROTTI), L.A.Grzelak@uu.nl (LECH A. GRZELAK)

The views expressed in this paper are the author's personal views and do not necessarily reflect the views or policies of their current or past employers. The authors have no competing interests.

An accompanying Python code to the article containing examples is available on [Github](#).

method [12], we will demonstrate a technique to improve the flexibility of the parametrizations by randomization one of the parameters to obtain a new parametrization with only limited additional parameters. The additional flexibility helps the parametrization to accurately model the market volatility when the classical parametrizations fail, such as before earnings announcements or generally for short-maturity options.

1.1. Problem Setting

We study the premium (or price) of a vanilla European option on an asset S with a predetermined expiry date T and strike price K . The price of such an option is written as

$$V_{c/p}(T, K) = BS_{c/p}(t_0, S_0, T, K; \hat{\sigma}(T, K)), \quad (1.1)$$

where $BS_{c/p}$ is the Black-Scholes formula for a call/put option and a constant risk-free rate r , $\hat{\sigma}(T, K) \geq 0$ is called the (*Black-Scholes*) *implied volatility* and S_0 the spot price of the asset. The Black-Scholes formula is a fundamental result in mathematical finance based on the Black-Scholes model, which assumes a lognormal probability distribution for the asset price process $S_t, t \geq t_0$. Since this assumption is known to be unrealistic, the Black-Scholes formula is most often used as a convenient way to quote prices of options available in the market as implied volatilities $\hat{\sigma}(T, K)$, rather than a pricing model. A market generally quotes options as implied volatilities on a discrete grid of strike prices and expiries. Suppose that Θ_{mkt} denotes a set of implied volatility quotes of the asset S for N expiries $\{T_1, T_2, \dots, T_N\}$ and M strikes $\{K_1, K_2, \dots, K_M\}$:

$$\Theta_{mkt} = \{\hat{\sigma}_{mkt}(T_n, K_m) : 1 \leq n \leq N, 1 \leq m \leq M\}. \quad (1.2)$$

Under the assumption of an efficient market, the market option quotes are set at a fair value based on market expectations of the future payoff. Practitioners are often interested in the price of an option for a pair (T, K) whose price $\hat{\sigma}_{mkt}(T, K) \notin \Theta_{mkt}$ is not in the commonly traded set, for instance, as market makers attempt to set fair option prices. Since the market does not directly provide this value, the objective is to extend Θ_{mkt} to a smooth function $\hat{\sigma}(T, K) : \Pi \rightarrow \mathbb{R}_+$ of implied volatilities, which provides such a quote for any pair on a desired domain $\Pi \subset (t_0, \infty) \times \mathbb{R}_+$. Since $\hat{\sigma}(T, K)$ is a smooth function in two variables, it defines a smooth surface on \mathbb{R}^3 and is therefore called the *implied volatility surface* (IV surface, or volatility surface). A primary condition of $\hat{\sigma}(T, K)$ is that the function is an extension of the discrete quotes, meaning that

$$\hat{\sigma}(T_n, K_m) = \hat{\sigma}_{mkt}(T_n, K_m), \quad 1 \leq n \leq N, 1 \leq m \leq M. \quad (1.3)$$

Secondly, the resulting volatility surface should at all times be free of static arbitrage opportunities. With the Black-Scholes equation, the volatility surface defines the theoretical prices for put and call options on the entire domain. If these option prices present arbitrage opportunities by buying or selling options with different strikes and expiries, the volatility surface is not deemed suitable since market participants could exploit these, thereby eliminating the opportunities. The absence of arbitrage is guaranteed by a number of conditions that can be equivalently formulated on the option prices or directly on the volatility surface [14].

Once the implied volatility function $\hat{\sigma}(T, K)$ is constructed from the market quotes and is arbitrage-free, it has various applications. Firstly, the option surface provides information on the market's expectation of the probability distribution of underlying asset S . For instance, the risk-neutral probability distribution of the asset S can be derived with the Breeden-Litzenberger formula [3], and the surface can be used to calibrate pricing models for exotic derivatives. Furthermore, the surface can be used for trading purposes by assessing volatility expectations, detecting arbitrage opportunities, or providing liquidity to the market.

1.2. Literature Review

Implied volatility surface modeling has been studied extensively in the past. Successful approaches have been developed using stochastic and local volatility models, statistical properties of the implied volatility surface, interpolation schemes, and, lately, machine learning. An

extensive review of the methods is found in [16]. We will quickly summarize the approaches that are relevant to our methodology.

The simplest way to obtain the function $\hat{\sigma}(T, K)$ is to choose an interpolation and extrapolation scheme to interpolate the available volatility quotes on the continuum. It is well known [7] that such an approach is not arbitrage-free since a direct interpolation on the volatility surface often leads to a non-convex option pricing function. The mispricing is further exaggerated for assets with few option quotes available in the market, where the interpolation determines a large portion of the surface, increasing the risk of generating implausible or arbitrageable prices. An arbitrage-free interpolation scheme is feasible on the option pricing function rather than the implied volatilities [18, 2]. The interpolation methods remain problematic for assets for which only a few high-quality option prices are available. Furthermore, to obtain the implied volatilities from the market prices, an inversion of the Black-Scholes formula is required, which can only be achieved by a root-finding algorithm.

The surfaces based on interpolation schemes have the feature that the market quotes Θ_{mkt} are always matched by $\hat{\sigma}(T, K)$ and therefore that (1.3) is true. The market quotes on the surface are fixed first, and the interpolated points are added in addition to completing the surface. *Volatility surface parametrizations* offer an alternative to this scheme. Rather than fixing the market quotes on the surface, the approach uses a fitting algorithm to choose the best-fitting surface from a predefined set of surfaces. First, a set of smooth surfaces $(T, K) \mapsto \hat{\sigma}(T, K; \bar{p})$ are defined by parameters $\bar{p} = (p_1, p_2, \dots, p_m)$. The parametrization is chosen so that the surface is always free of arbitrage. The domain of the parameter space defines the set of all possible surfaces that can be created. The implied volatility surface for an asset S is then chosen such that the difference to the market quotes Θ_{mkt} is minimized. While the surface will not exactly match Θ_{mkt} , the difference is negligible if the space of possible surfaces is “large” enough.

Volatility parametrizations are often directly derived from a parametric asset model, such as a stochastic volatility model. Although a volatility surface can be generally derived for any asset price model, not all models offer a convenient analytical form for the volatility surface. Defining an analytically tractable and realistic model (in terms of fitting the market) is thus a challenging task. The *Stochastic Volatility Inspired (SVI)* parametrization [9] was derived from a stochastic volatility model and enjoyed great success in the past. The parametrization was extended and improved in multiple works [19, 6]. Another successful parametrization is the *SABR parametrization* [15], a direct result of the Hagan et al. formula provided by the SABR model (Stochastic-Alpha-Beta-Rho). Parametric volatility surfaces are convenient for numerous reasons. Firstly, since the parametrizations are derived from an asset model, the absence of arbitrage is guaranteed as long as the parameters remain in a well-defined range. Simple constraints on the parameter space are usually sufficient to ensure the absence of arbitrage. Secondly, the parameters can be attributed to the shape of the volatility surface. This allows for a simple way to compare surfaces and the expression of the dynamics of the surface in terms of the dynamics of the parameter. Thirdly, theoretically, no minimum number of market quotes is required to fit an arbitrage-free surface. Although a higher number of quotes is desired for stability in the calibration, a parametrization can be fit to any number of quotes and remain arbitrage-free. This is of particular importance for assets with only a few quotes or only in a particular strike region, where little to no information is provided for the tails of the volatility curves.

The main drawback of parametrizations is that there is no guarantee that a surface that is appropriately close to the market data can be found. The flexibility of the surface is limited by the chosen parametrization, which does not cover all viable (i.e. arbitrage-free) volatility shapes. If the market conditions are not within the scope of the parametrization, the fitting process fails, and the parametrization misrepresents the actual market conditions. These out-of-scope market conditions can be systemic, meaning that parametric models are generally unfit to model a certain market behavior. For instance, it is well-known that short-maturity options in equity markets exhibit a steeper at-the-money implied volatility term structure than attainable under regular stochastic volatility models [8]. Alternatively, the market condition can be out of scope due to an irregular behavior in the market, such as spikes in volatility or higher-than-usual uncertainty. It is not uncommon for very short-term options markets (near expiry) to exhibit a W-shaped volatility shape, or “mustache” shapes [10] before an earnings

announcement of the underlying equity. These shapes of volatility surface arise from *bimodal* risk-neutral probability density functions for the stock price, which reflect the dichotomous nature of the earnings, which can either have a positive or negative effect on the asset price. Classical diffusion models¹ are unable to create such shapes due to the single continuous diffusive driver, and the corresponding volatility parametrization is limited in such cases. This limitation highlights the industry’s need for more flexible parameterized surfaces to achieve better fits in such market situations.

1.3. Contributions

In this paper, we study volatility surfaces in cases when the parametric surfaces reach the limit of their flexibility. We introduce a generic method to enhance the flexibility in such cases using a randomization scheme of the parameters of the surface. By replacing one or more parameters of the parametric surface with a random variable, we derive a new implied volatility surface with increased flexibility to fit the market. The new randomized volatility surface is expressed in terms of the original parameters plus parameters to specify the chosen random variable. To show the effectiveness of the novel method, we apply the method to the existing parametrizations of the SABR parametrization and demonstrate that the additional flexibility enables them to better fit the market data for SPX options with expiry dates of less than half a year. Furthermore, we derive a second kind of randomization where we randomize the spot price S_0 of the asset. This arbitrage-free randomization is shown to be particularly effective for near-maturity options (i.e., options with an expiry date in the next few days) before an earning announcement, which induces a multi-modal-type volatility regime.² The paper is organized in the following way: Section 2 describes the process of randomizing a parametrization of volatility surfaces and proves that the randomization is indeed free of static arbitrage. We present a few examples of randomized parametrizations and their effectiveness in Section 3.2. In particular, we show an improved fit to options on the S&P 500 index. In Section 4, we then introduce the randomized spot parametrization and also present an example of its use on short-maturity AMZN options on the day of an earnings announcement. Finally, we conclude the paper in Section 5.

2. Parameter Randomization and Analytical Implied Volatility

2.1. General Volatility Parametrizations

We consider a type of implied volatility surfaces, which are given in parametric form, defined by a set of parameters. As a starting point, suppose that $\bar{p} := (p_1, \dots, p_m)$ is an array of m constant parameters on a parameter domain $\bar{p} \in \mathcal{D} \subset \mathbb{R}^m$. We define a *parameterized implied volatility function* as a positive function

$$\hat{\sigma}(T, K; \bar{p}) := \hat{\sigma}(T, K; (p_1, \dots, p_m)) \geq 0, \quad (2.1)$$

of expiry and strike price $(T, K) \in \Pi = (t_0, \infty) \times [0, \infty)$ given the associated parameters p_1, \dots, p_m . The map $\hat{\sigma}(T, K; \bar{p})$ for a fixed \bar{p} is referred to as a *parameterized implied volatility surface*³ since the set

$$\{(T, K, \hat{\sigma}(T, K; \bar{p})) : (T, K) \in \Pi\} \subset \mathbb{R}^3, \quad (2.2)$$

defines a surface over the domain Π . The exact shape of the surface depends on the parameters \bar{p} and the chosen parametrization function. Since the parameterized implied volatility function is positive, we can compose the function with the Black-Scholes formula and obtain the *parametrized (put/call) pricing function*, defined as

$$V_{c/p}(T, K; \bar{p}) := BS_{c/p}(t_0, S_0, T, K; \hat{\sigma}(T, K; \bar{p})),$$

¹It needs to be mentioned that SVI-type parametrizations do not rely on the an underlying model, but their development was merely inspired by volatility shapes of the Heston model. Nevertheless, one observes the same characteristics in terms of fit as classical stochastic volatility models.

²We speak of a multi-modal-type volatility regime when the risk-neutral probability density functions implied by the volatility surface exhibit more than one mode, and are therefore *multi-modal*.

³Sometimes we refer to the function as *parametric volatility surface* or simply *parametrization*.

for an asset with spot price S_0 at t_0 . The function provides a continuum of European call and put option prices on the underlying asset on $(t_0 \times \infty) \times [0, \infty)$ given the implied volatility $\hat{\sigma}(T, K; \bar{p})$. We can extend the functions to the limit points at $T = t_0$, which, under certain conditions, exist and are given by $V_c(t_0, K; \bar{p}) = (S_0 - K)^+$ and $V_c(t_0, K; \bar{p}) = (K - S_0)^+$ (see Definition 2.1). The pricing function defines two additional surfaces in \mathbb{R}^3 over the domain Π , which we refer to as the (put/call) pricing surface.

Since the parameterized implied volatility and pricing surface define a set of prices for tradable options, these prices must be free of arbitrage opportunities. There are various ways to define the absence of arbitrage of an implied volatility surface, most of which are equivalent. Here, we will utilize the *model-free* definition [21], which does not rely on the introduction of stochastic asset models but can be expressed as a set of conditions on the pricing surfaces.

Definition 2.1 (Arbitrage-free volatility surface). *Given a set of parameters \bar{p} , let $\hat{\sigma}(T, K; \bar{p})$ be a parameterized implied volatility surface defined on $\Pi = \Pi_T \times \Pi_K = (t_0, \infty) \times \mathbb{R}_+$. Let $V_c(T, K; \bar{p})$ be its call pricing function, which is extended to the limit points at $T = t_0$. The parametrization is called free of “butterfly” arbitrage if the following conditions hold on the call pricing function and a constant $s > 0$:*

- i) $V_c(T, \cdot; \bar{p})$ is convex and non-increasing for all $T \in \Pi_T$.
 - ii) $\lim_{K \rightarrow \infty} V_c(T, K; \bar{p}) = 0$ for all $T \in \Pi_T$.
 - iii) $(s - K)^+ \leq V_c(T, K; \bar{p}) \leq s$ for all $(T, K) \in \Pi$.
 - iv) $V_c(t_0, K; \bar{p}) = (s - K)^+$ for all $K \in \Pi_K$.
- If the following additional condition holds, the pricing surface is also free of “calendar” arbitrage, and we call the surface arbitrage-free:
- v) $V_c(\cdot, K; \bar{p})$ is non-decreasing for all $K \in \Pi_K$.

Equivalent conditions in terms of the put-call parity can be derived for the put pricing function $V_p(T, K; \bar{p})$, or directly in terms of the volatility surface $\hat{\sigma}(T, K; \bar{p})$ [14]. Under these conditions, one can prove the existence of a non-negative local martingale process on a suitable probability space such that the call price function can be written as a risk-neutral expectation of the final payoff. In other words, an arbitrage-free model (price process) exists that yields the volatility surface. However, we will not utilize this fact to avoid introducing any model dynamics and remain “model-free”.

Due to the continuity of the Black-Scholes formula with respect to the volatility input, and the conditions above, it is necessary for the parameterized volatility function and parameterized price function $V_{c/p}(T, K; \bar{p})$ to be $C^{1,2}$, meaning that the price and volatility surfaces are both smooth. Therefore, one can obtain the risk-neutral probability density functions $\{p_{S_t} : t \geq t_0\}$, defined as⁴

$$p_{S_t}(x) := e^{r(t-t_0)} \frac{d^2 V_c(t, x; \bar{p})}{dx^2}, \quad (2.3)$$

for any $t \geq t_0$ using the Breeden-Litzenberger formula [3] and risk-free rate r . In particular, one can show with a few manipulations that expected value of the random variable S_t whose PDF is given by is $p_{S_t}(\cdot)$, is

$$\mathbb{E}[S_t] = S_0 e^{r(t-t_0)}. \quad (2.4)$$

Conversely, given a set of PDFs, such that (2.4) holds for all $t \geq t_0$, we can define an arbitrage-free pricing surface by integration of the probability densities [9].

If considering an implied volatility surface at a fixed expiry $T \in \Pi_T$, we refer to the resulting function $\hat{\sigma}_T(K; \bar{p}) := \hat{\sigma}(T, K; (p_1, \dots, p_m))$ as an *implied volatility slice*. Furthermore, we denote the collection of all possible volatility surfaces \mathcal{S} for a parametrization as

$$\mathcal{S} := \{\hat{\sigma}(T, K; \bar{p}) : \bar{p} \in \mathcal{D}\}. \quad (2.5)$$

⁴Note that one can also use the put prices $V_p(t, x; \bar{p})$ to obtain the same result.

To obtain a volatility surface that fits the market, we find the optimal parameters \bar{p} , which minimizes the difference between the market quotes

$$\bar{p}_{opt} = \arg \min_{\hat{\sigma}(T, K; \bar{p}) \in \mathcal{S}} \sum_{i,j}^{N,M} \|\hat{\sigma}(T_i, K_j; \bar{p}) - \sigma_{mkt}(T_i, K_j)\|, \quad (2.6)$$

with respect to a desired norm $\|\cdot\|$. The ability to fit the market, therefore, directly depends on the “size” of \mathcal{S} , whether \mathcal{S} contains a function that can match the market.

2.2. Volatility Parametrizations with Random Parameters

In an effort to increase the size of \mathcal{S} and obtain better fitting arbitrage-free volatility surfaces, we consider the possibility of adding stochasticity to the implied volatility surface by replacing one of the parameters p_i for $1 \leq i \leq m$ with a random variable. Let $\hat{\sigma}(T, K; \bar{p})$ be a parameterized implied volatility function with parameter domain $\mathcal{D} \subset \mathbb{R}^m$ and suppose that ϑ is an absolutely continuous real-valued random variable on a probability space $(\Omega, \mathcal{F}, \mathbb{P})$ with associated probability density function $f_\vartheta(\cdot)$. We can replace the i -th entry of \bar{p} with the random variable ϑ to obtain the random vector $\bar{p}(\vartheta) = (p_1, p_2, \dots, \vartheta, \dots, p_m)$. If we assume that $\bar{p}(\vartheta)$ is almost surely in the domain \mathcal{D} , a realization $\omega \in \Omega$ determines a real-valued vector $\bar{p}(\theta) := (p_1, p_2, \dots, \theta, \dots, p_m) \in \mathbb{R}^m$ with $\theta = \vartheta(\omega)$, which almost surely provides an arbitrage-free implied volatility surface $\hat{\sigma}(T, K; \bar{p}(\theta))$ and its associated pricing functions $V_{c/p}(T, K; \bar{p}(\theta))$.

Assuming measurability of the parametrization function in the parameters, the pricing function $V_{c/p}(T, K; \bar{p}(\vartheta))$ is thus a random variable, and we can compute the expectation

$$\mathbb{E}[V_{c/p}(T, K; \bar{p}(\vartheta))] = \int_{\mathbb{R}} BS_{c/p}(t_0, S_0, T, K; \hat{\sigma}(T, K; \bar{p}(\theta))f_\vartheta(\theta)d\theta, \quad (2.7)$$

where f_ϑ is the associated probability density function of ϑ . The equation shows that the expected option price under the randomized volatility surface is effectively an average of option prices on the sample space of the parameters of the volatility surface. Since the expectation of the randomized pricing function is a deterministic function in two variables, we can investigate its suitability to be a pricing function. Due to the linear properties of probability density functions, the function is indeed an arbitrage-free pricing function.

Lemma 2.2 (Arbitrage-free randomization). *Let $\hat{\sigma}(T, K; \bar{p})$ be an arbitrage-free parameterized implied volatility function on the parameter domain $\bar{p} \in \mathcal{D}$ and let ϑ be a real-valued absolutely continuous random variable. Suppose that $\bar{p}(\vartheta) = (p_1, p_2, \dots, \vartheta, \dots, p_m)$ is the random vector where we replaced the i -th parameter of \bar{p} with ϑ . Then, the map $\hat{\sigma}(T, K)$ such that*

$$BS_{c/p}(t_0, S_0, T, K; \hat{\sigma}(T, K)) = \mathbb{E}[V_{c/p}(T, K; \bar{p}(\vartheta))], \quad \forall (T, K) \in \Pi, \quad (2.8)$$

is an arbitrage-free implied volatility surface. We refer to $\hat{\sigma}(T, K)$ as a randomization of $\hat{\sigma}(T, K; \bar{p})$ with random variable ϑ in parameter i .

Proof. The conditions of an arbitrage-free surface are given by Definition 2.1, and it is possible to prove the lemma by confirming that each condition is closed under convex combinations. We will show separately that the surface is free of butterfly arbitrage and free of calendar arbitrage. The first step is thus to confirm that for each fixed $T \in \Pi_T$, the volatility slice $\hat{\sigma}_T(K)$ is arbitrage-free. We recall that the call price can be written as an integration of the risk-neutral PDF $p_{S_T; \theta}$

$$V_{c/p}(T, K; \bar{p}(\theta)) = e^{-r(T-t_0)} \int_K^\infty (x - K) p_{S_T; \theta}(x) dx.$$

The expectation can thus be written as

$$\begin{aligned} \mathbb{E}[V_c(T, K; \bar{p}(\vartheta))] &= \int_{\mathbb{R}} V_c(T, K; \bar{p}(\theta)) f_\vartheta(\theta) d\theta \\ &= \int_{\mathbb{R}} e^{-r(T-t_0)} \int_K^\infty (x - K) p_{S_T; \theta}(x) dx f_\vartheta(\theta) d\theta \\ &= e^{-r(T-t_0)} \int_K^\infty (x - K) \int_{\mathbb{R}} p_{S_T; \theta}(x) f_\vartheta(\theta) d\theta dx. \end{aligned}$$

Since the random vector $\bar{p}(\vartheta)$ takes values almost surely in \mathcal{D} , the function $p_{S_T; \theta}(\cdot)$ is a proper probability density function when $f_\vartheta(\theta) > 0$. The expression $\int_{\mathbb{R}} p_{S_T; \theta}(x) f_\vartheta(\theta) d\theta$ is a convex combination of probability densities (mixture density), which we define as the function

$$\bar{f}(x) := \int_{\mathbb{R}} p_{S_T; \theta}(x) f_\vartheta(\theta) d\theta,$$

We claim $\bar{f}(x)$ to be a proper probability density function on $[0, \infty)$. The function $\bar{f}(x)$ is certainly positive since $p_{S_T; \theta}(\cdot)$, $f_\vartheta(\cdot)$ are positive functions, and integrates to 1 since

$$\begin{aligned} \int_0^\infty \bar{f}(x) dx &= \int_0^\infty \int_{\mathbb{R}} p_{S_T; \theta}(x) f_\vartheta(\theta) d\theta dx \\ &= \int_{\mathbb{R}} \int_0^\infty p_{S_T; \theta}(x) dx f_\vartheta(\theta) d\theta \\ &= \int_{\mathbb{R}} f_\vartheta(\theta) d\theta \\ &= 1. \end{aligned}$$

This proves the claim and is a sufficient condition for $\hat{\sigma}_T(K)$ to be butterfly-arbitrage-free [9]. It remains to show that condition v) is true as well. Let K be fixed and suppose that $t_1 < t_2 \in \Pi_T$. Since $\hat{\sigma}(T, K; \bar{p}(\vartheta))$ is arbitrage-free, we have that $V_c(t_1, K; \bar{p}(\vartheta)) \leq V_c(t_2, K; \bar{p}(\vartheta))$ for $\bar{p}(\vartheta) \in \mathcal{D}$. Since this is almost surely the case, we conclude that

$$\mathbb{E}[V_c(t_1, K; \bar{p}(\vartheta))] \leq \mathbb{E}[V_c(t_2, K; \bar{p}(\vartheta))],$$

and therefore, that condition v) is fulfilled, too. \blacksquare

The map $\hat{\sigma}(T, K)$ as defined Equation (2.8) is thus an arbitrage-free implied volatility surface, and the pricing of European-style options will collapse to determining a mixture distribution weighted with the probability distribution of ϑ . If we specify the probability distribution of the random variable ϑ in parametric form, we can combine the sets of the parametrized surface and the random variable to a common set of parameters. Suppose that the random variable ϑ is given in parametric form by the parameters $\bar{q} = (q_1, q_2, \dots, q_l) \in \mathbb{R}^l$. We combine the parameter sets of \bar{q} and \bar{p} to an extended parameter parameter vector

$$\bar{p}^* = (p_1, p_2, \dots, p_{i-1}, p_{i+1}, \dots, p_m, q_1, \dots, q_l) \in \mathcal{D}^*, \quad (2.9)$$

where \mathcal{D}^* is a new parameter space. The map $\hat{\sigma}(T, K) := \hat{\sigma}(T, K; \bar{p}^*)$ therefore regains a parameterized form.

Example 2.1. We clarify the notation of the extended parameter space \mathcal{D}^* on a simple example of a randomization. Suppose that $\hat{\sigma}(T, K, (a, b, c))$ is a parametric implied volatility surface with domain $(a, b, c) \in \mathcal{D} = \mathbb{R}^3$. We consider a randomization of $\hat{\sigma}(T, K, (a, b, c))$ in parameter c with the normally distributed random variable $\vartheta \sim \mathcal{N}(\mu, \nu)$ for $(q_1, q_2) = (\mu, \nu) \in \mathbb{R} \times \mathbb{R}_+$. This randomization is thus given in parametric form by the function $\hat{\sigma}(T, K, \bar{p}^*)$ for the parameters

$$\bar{p}^* = (a, b, \mu, \nu) \in \mathcal{D}^* = \mathbb{R}^3 \times \mathbb{R}_+.$$

The definition of $\hat{\sigma}(T, K, \bar{p}^*)$ is given by (2.8).

Since we defined $\hat{\sigma}(T, K, \bar{p}^*)$ in terms of the pricing surface and the Black-Scholes formula has no analytical inverse in the volatility parameter, we no longer have an analytical expression of the volatility surface. However, it is possible to derive an analytic expansion of the implied volatility surface, which we aim to derive step by step for the remainder of the section.

As the pricing surface of the randomized parametrization $V_{c/p}(T, K; \bar{p}^*)$ is defined as an integral over the domain of parameters, weighted by the PDF of the random variable ϑ , we discretize the integral using a numerical integration scheme. We have to ensure that the discretization is arbitrage-free, for which we utilize an integration technique that maintains the convex property of the summation. The Gaussian quadrature integration approximates an

integral of the form $\int_a^b h(x)w(x)dx$, on a real domain $[a, b] \subset \mathbb{R}$, for an integrable function $h(x)$ and a weight function $w(x)$, as the sum

$$\int_a^b h(x)w(x)dx \approx \sum_{n=1}^{N_q} \lambda_n h(x_n), \quad (2.10)$$

where $\{\lambda_n, \theta_n\}_{n=1}^{N_q}$ are called Gauss-quadrature weights. The important property of the Gauss-quadrature integration is that the integral is exact for any polynomial of degree less than $2N_q$. Since the expression $h(x) = 1$ is a polynomial of degree 0, the approximation is exact for this integrate and we obtain

$$\int_a^b 1w(x)dx = \int_a^b w(x)dx = \sum_{n=1}^{N_q} \lambda_n. \quad (2.11)$$

The weights of a Gaussian quadrature approximation thus always sum 1. If we apply the integration technique to the randomized price surface with $w(x) = f_\vartheta(x)$, we obtain that

$$V_{c/p}(T, K; \bar{p}^*) = \int_{\mathbb{R}} V_{c/p}(T, K; \bar{p}(\theta)) f_\vartheta(\theta) d\theta \approx \sum_{n=1}^{N_q} \lambda_n V_{c/p}(T, K; \bar{p}(\theta_n)), \quad (2.12)$$

where the pairs $\{\lambda_n, \theta_n\}_{n=1}^{N_q}$ are the Gauss-quadrature weights and nodes. These weights and nodes depend on the distribution function $F_\vartheta(\cdot)$ of ϑ and can be calculated explicitly as outlined in [Appendix A](#). We define the *truncated*, or *discretized pricing surface* with N_q terms as the sum

$$V_{c/p}(T, K; \bar{p}^*, N_q) := \sum_{n=1}^{N_q} \lambda_n V_{c/p}(T, K; \bar{p}(\theta_n)). \quad (2.13)$$

Since the discretization is only an approximation of $V_{c/p}(T, K; \bar{p}^*, N_q)$ we have to ensure that it is arbitrage-free too.

Lemma 2.3. *Let $V_{c/p}(T, K; \bar{p}^*)$ be a randomized pricing surface for a parametrization $\hat{\sigma}(T, K; \bar{p})$ with random variable ϑ in a parameter $i \leq m$. Let $V_{c/p}(T, K; \bar{p}^*, N_q)$ be the discretized pricing surface of the randomization. Then, there is a discrete random variable $\bar{\vartheta}$, which defines a randomization of $\hat{\sigma}(T, K; \bar{p})$ in parameter i with the property that*

$$\mathbb{E}[V_{c/p}(T, K; \bar{p}(\bar{\vartheta}))] \equiv V_{c/p}(T, K; \bar{p}^*, N_q). \quad (2.14)$$

This implies in particular that $V_{c/p}(T, K; \bar{p}^*, N_q)$ is an arbitrage-free pricing surface.

Proof. Let $\{\lambda_n, \theta_n\}_{n=1}^{N_q}$ be the Gauss-quadrature pairs of ϑ of degree N_q and define the function $f_{\bar{\vartheta}}(\cdot): \mathbb{R} \rightarrow \mathbb{R}_+$ such that

$$f_{\bar{\vartheta}}(x) = \begin{cases} \lambda_n, & \text{if } x = \theta_n, \\ 0 & \text{otherwise.} \end{cases}$$

We claim that this is a probability mass function. Since $\lambda_n \geq 0$ for all $n \leq N_q$, the function is certainly positive. Furthermore, since quadrature integration is exact for polynomials up to $2N_q$ degree, we have as in (2.11), that $\int_{\mathbb{R}} f_{\bar{\vartheta}}(x)dx = 1$. By Skorohod's representation theorem, there exists a random variable $\bar{\vartheta}$, such that $f_{\bar{\vartheta}}$ is its probability mass function. It follows that (2.14) is true, since $\mathbb{E}[V_{c/p}(T, K; \bar{p}(\bar{\vartheta}))]$ is given by $\sum_{n=1}^{N_q} \lambda_n V_{c/p}(T, K; \bar{p}(\theta_n))$. \blacksquare

Remark (Choice of N_q). *Generally, a larger choice of N_q means that the discretized randomization approximates the continuous randomization better. However, since the discretization is arbitrage-free for any $N_q \in \mathbb{N}$, an exact approximation of a continuous ϑ is not necessary, and N_q can be treated simply as a parameter to further specify the nature of the randomization of the parameters.*

2.3. Analytic Expansion of Randomized Volatility Surface

With the additional parameter and the help of the quadrature integration, we transformed the semi-analytical pricing surface into a finite sum of prices given by the discretized randomization of (2.13). Since the Black-Scholes equation has no analytical inverse in the volatility argument, the implied volatility surface $\hat{\sigma}(T, K; \bar{p}^*, N_q)$ cannot be obtained explicitly. Nevertheless, Brigo and Mercurio [4] showed how to get a polynomial expansion of the implied volatility function based on the Taylor expansion under a mixture model of lognormal prices. We derive a generalization of this result, and we use it to obtain an analytic expression of $\hat{\sigma}(T, K; \bar{p}^*, N_q)$. Let $(T, K) \in \Pi$ be fixed and suppose we want to find the value of $\hat{\sigma}(T, K; \bar{p}^*, N_q)$. We first define the function $m(T, K)$ as

$$m(T, K) := \log \frac{S_0}{K} + rT, \quad (2.15)$$

where r is the interest rate. Furthermore, let $P(m): \mathbb{R} \rightarrow \mathbb{R}_+$ a positive, continuously differentiable function of one variable m , for which we define the value at $m = m(T, K)$ as $P(m(T, K)) = \hat{\sigma}(T, K; \bar{p}^*, N_q)$. The Black-Scholes price of an option at (T, K) with implied volatility $P(m(T, K))$ can be written as a function f , such that

$$f(m, P(m)) := S_0 \left[\Phi \left(\frac{m + \frac{1}{2}\hat{\sigma}^2(m)T}{P(m)\sqrt{T}} \right) - e^{-m} \Phi \left(\frac{m - \frac{1}{2}\hat{\sigma}^2(m)T}{P(m)\sqrt{T}} \right) \right]. \quad (2.16)$$

On the other hand, a discretized price surface $V_{c/p}(T, K; \bar{p}^*, N_q)$ with $\eta_n = \hat{\sigma}(T, K, \bar{p}(\theta_n))$ can be written as a function of m as well. We define:

$$g(m) := S_0 \sum_{n=1}^{N_q} \lambda_n \left[\Phi \left(\frac{m + \frac{1}{2}\eta_n^2 T}{\eta_n \sqrt{T}} \right) - e^{-m} \Phi \left(\frac{m - \frac{1}{2}\eta_n^2 T}{\eta_n \sqrt{T}} \right) \right]. \quad (2.17)$$

If we equate the two equations, since $P(m(T, K))$ is equal to $\hat{\sigma}(T, K, \bar{p}(\theta_n))$, the equation

$$f(m, \hat{\sigma}(m)) = g(m), \quad (2.18)$$

is exactly equal to (2.13) at $m = m(T, K)$. The goal is to obtain a polynomial expansion of the function $P(m)$, which we can then evaluate at $m = m(T, K)$ to obtain the randomized volatility function at (T, K) . The expansion utilizes the ideas from the implicit function theorem [17] to obtain any higher-order derivative from an implicit function, such as Equation (2.18). We can obtain the derivatives of $P(m)$ by differentiating both sides with respect to m and write the function $P(m)$ as a Taylor expansion in terms of the derivatives at 0 and the function $P(m)$ at $m = 0$.

Theorem 2.4. *Let $\hat{\sigma}(T, K; \bar{p})$ be an implied volatility parametrization on the parameter domain \mathcal{D} , which is continuously differentiable in T and K , and let $\hat{\sigma}(T, K; \bar{p}^*, N_q)$ with $\bar{p}^* \in \mathcal{D}^*$ be its discretized randomization with the quadrature points $\{\lambda_n, \theta_n\}_{n=1}^{N_q}$. Let*

$$m(T, K) := \log \frac{S_0}{K} + rT,$$

be the log-moneyness with interest-rate r . Then, the discretized randomization $\hat{\sigma}(T, K; \bar{p}^, N_q)$ at (T, K) is given by the Taylor expansion $P_{(T, K)}(m): \mathbb{R} \rightarrow \mathbb{R}$, evaluated at $m = m(T, K)$, where*

$$P_{(T, K)}(m) = P_{(T, K)}(0) + \frac{P_{(T, K)}^{(2)}(0)}{2!} m^2 + \frac{P_{(T, K)}^{(4)}(0)}{4!} m^4 + \frac{P_{(T, K)}^{(6)}(0)}{6!} m^6 + \mathcal{O}(m^8), \quad (2.19)$$

such that the expansion terms are given by

$$P_{(T, K)}(0) = \frac{2}{\sqrt{T}} \Phi^{-1} \left(\sum_{n=1}^{N_q} \lambda_n \Phi \left(\frac{1}{2} \eta_n \sqrt{T} \right) \right),$$

$$\begin{aligned}
P_{(T,K)}^{(2)}(0) &= \frac{1}{2\sqrt{T}} \left\{ -\frac{1}{\Sigma_0} + \sum_{n=1}^{N_q} \lambda_n \frac{E_n}{H_n} \right\}, \\
P_{(T,K)}^{(4)}(0) &= \frac{1}{8\sqrt{T}} \left\{ \frac{1 + 6\Sigma_2 + \Sigma_0^2(-7 - 6\Sigma_2 + 3\Sigma_2^2)}{\Sigma_0^3} + \sum_{n=1}^{N_q} \lambda_n \left[\frac{E_n}{H_n^3} (-1 + 7H_n^2) \right] \right\}, \\
P_{(T,K)}^{(6)}(0) &= \frac{1}{32\sqrt{T}} \left\{ \frac{-3 - 45\Sigma_2 + \Sigma_0^2(90\Sigma_2 + 60\Sigma_4) + \Sigma_0^4\Sigma_2(45\Sigma_2 + 60\Sigma_4 - 15\Sigma_2^2)}{\Sigma_0^5} \right. \\
&\quad \left. + \frac{16\Sigma_0^2 - 90\Sigma_2^2 - 31\Sigma_0^4 - 45\Sigma_0^2\Sigma_2^2 - \Sigma_0^4(15\Sigma_2 + 60\Sigma_4) + 15\Sigma_0^2\Sigma_2^3}{\Sigma_0^5} \right. \\
&\quad \left. + \sum_{n=1}^{N_q} \lambda_n \left[\frac{E_n}{H_n^5} (3 - 16H_n^2 + 31H_n^4) \right] \right\},
\end{aligned}$$

with the auxiliary quantities:

$$\begin{aligned}
\Sigma_0 &:= \frac{1}{2} P_{(T,K)}(0)\sqrt{T}, & \Sigma_2 &:= P_{(T,K)}(0)P_{(T,K)}^{(2)}(0)T, & \Sigma_4 &:= P_{(T,K)}(0)P_{(T,K)}^{(4)}(0)T, \\
H_n &:= \frac{1}{2}\eta_n\sqrt{T}, & E_n &:= \exp\left(\frac{1}{2}(\Sigma_0^2 - H_n^2)\right), & \eta_n &= \hat{\sigma}(T, K; \bar{p}(\theta_n)).
\end{aligned}$$

The expression $\mathcal{O}(m^8)$ is the usual Big-O notation as $m \rightarrow 0$, meaning that for the remainder $R(m)$ we have $\lim_{x \rightarrow 0} \frac{R(m)}{m^8} \leq C$ for some constant C .

Proof. Let $(T, K) \in \Pi$ be fixed. We consider the following equation:

$$f(m, P_{(T,K)}(m)) = g(m), \quad (2.20)$$

with f, g given as above, and $P_{(T,K)}(m)$ a continuously differentiable function, such that $P_{(T,K)}(m(T, K)) = \hat{\sigma}(T, K; \bar{p}^*, N_q)$. The values of $P_{(T,K)}$ are defined through the functional equation. Since the inverse of $f(\cdot)$ in the second variable is unknown, it is not possible to explicitly express $P_{(T,K)}$ in analytical form, but we apply the technique of *implicit differentiation* to derive a polynomial expansion for it. Differentiating both sides of the Equation (2.20), we have

$$f_x(m, P_{(T,K)}(m)) + f_y(m, P_{(T,K)}(m))P'_{(T,K)}(m) = g'(m),$$

where f_x, f_y are the partial derivatives of f with respect to the first and second input variable. In the domain $D_0 := \{m \in \mathbb{R} | f_y(m, P_{(T,K)}(m)) \neq 0\}$ we can write:

$$P'_{(T,K)}(m) = \frac{g'(m) - f_x(m, P_{(T,K)}(m))}{f_y(m, P_{(T,K)}(m))}, \quad m \in D_0.$$

We can now obtain any order derivative of $P_{(T,K)}(m)$ by differentiating both sides by m and express the n -order derivatives of $P_{(T,K)}(m)$ as partial derivatives of f of at most n degrees. Note, however, that the number of derivatives on the right-hand side grows exponentially⁵ in the order of the target derivative (due to the *formula of the derivation of a product*). As it turns out, all the second-order derivatives disappear, simplifying the calculation significantly.

Finally, we obtain the expansion by combining the terms and evaluating $P_{(T,K)}(m)$ at $m = 0$:

$$f(0, P_{(T,K)}(0)) = S_0 \left[\Phi(P_{(T,K)}(0)\sqrt{T}) - \Phi(-P_{(T,K)}(0)\sqrt{T}) \right],$$

and

$$g(0) = S_0 \sum_{n=1}^{N_q} \lambda_n \left[\Phi(\eta_n\sqrt{T}) - \Phi(-\eta_n\sqrt{T}) \right],$$

⁵More precisely, the growth is exponentially bounded from above (by 2^{i-1} with $i > 0$ the order of differentiation). It is possible to reorder and collect the terms in such a way the overall number is slightly lower, but in any case, the growth is “more than” polynomial.

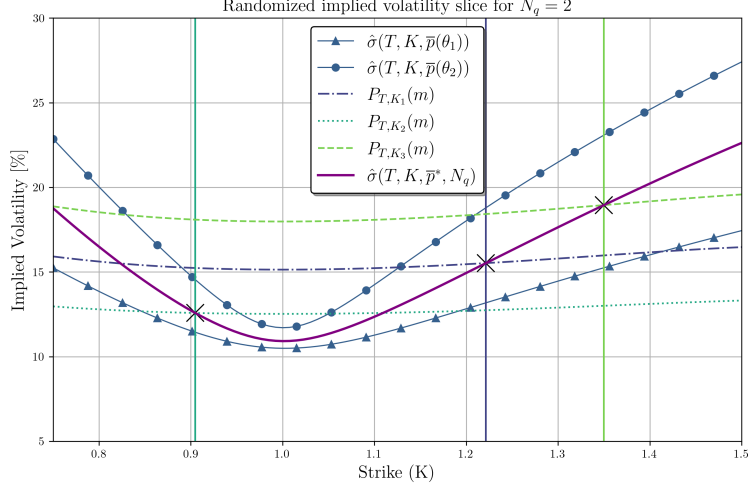


Figure 1: The figure shows the randomization of a parametrization with $N_q = 2$ for a fixed time T . The grey plots show the individual slices which are mixed, and the green lines show the function $P_{(T,K)}$ for three different K s. For each $P_{(T,K)}$, the randomized volatility meets the expansion $P_{(T,K_i)}$ exactly at K_i .

from which we obtain

$$P_{(T,K)}(0) = \frac{2}{\sqrt{T}} \Phi^{-1} \left(\sum_{n=1}^{N_q} \lambda_n \Phi \left(\frac{1}{2} \eta_n \sqrt{T} \right) \right).$$

Combining the results, we can express the function $P_{(T,K)}(m)$ as its Taylor expansion function around 0, which yields (2.19), and obtain the value for $\hat{\sigma}(T, K; \bar{p}^*, N_q)$ by evaluating at $m(T, K)$. \blacksquare

The expansion formula completes the process of obtaining the randomized surface from a regular parametrization of a volatility surface. A graphical representation of the expansions is shown in Figure 1. We also summarize the steps of the randomization in Figure 2, which provides an overview of the entire process from the initial parametrization to the randomized parametrization.

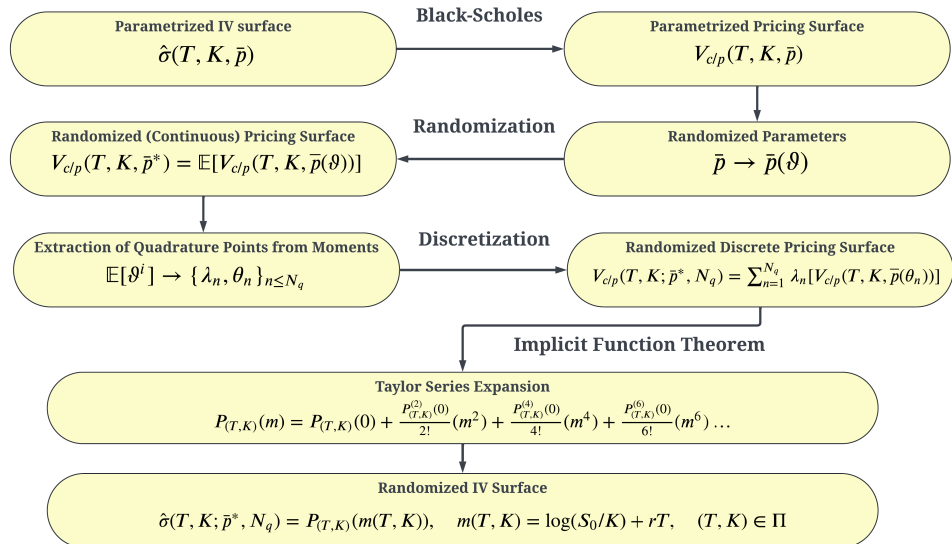


Figure 2: Process of randomization in steps

3. Illustrative Examples

The process of randomization transforms a parametric implied volatility surface into a new parametric implied volatility surface with extra parameters and flexibility. We examine a few examples of this randomization process to better understand its mechanics and effectiveness.

3.1. Randomized Flat Volatility

We start by examining the most trivial example of a parametrization, which we call the *flat parametrization*. This parametrization is given as the constant function $\hat{\sigma}(T, K; \sigma) = \sigma$, where $\sigma \geq 0$. Since the parametrization is independent of time T and strike K , the resulting implied volatility surface is a flat plane with a level of σ , and the parameter space \mathcal{D} is given by $\mathcal{D} = [0, \infty)$. This parametrization is equivalent to pricing options under the Black-Scholes model with volatility σ , which is known to not fit well to usual market conditions. We aim to increase its flexibility by randomizing the parameter σ and substituting it with a suitable random variable ϑ . Since σ must be positive, the random variable ϑ must be chosen almost surely positive. We propose that ϑ follows a log-normal distribution with mean μ and variance ν^2 , such that $\log(\vartheta) \sim \mathcal{N}(\mu, \nu^2)$ for some parameters μ, ν in the new parameter space $\mathcal{D}^* = \mathbb{R} \times [0, \infty)$. The randomized pricing surface is then given by Equation (2.12), a mixture of Black-Scholes prices weighted by the probability density function of the lognormal distribution

$$V_{c/p}(T, K; (\mu, \nu)) = \mathbb{E}[V_{c/p}(T, K; \vartheta)] = \int_0^\infty BS_{c/p}(t_0, S_0, T, K; \sigma) f_{LN(\mu, \nu^2)}(\sigma) d\sigma, \quad (3.1)$$

where

$$f_{LN(\mu, \nu^2)}(x) = \frac{1}{x\nu\sqrt{2\pi}} \exp\left(-\frac{(\log x - \mu)^2}{2\nu^2}\right). \quad (3.2)$$

We obtain the discretized randomization price $V_{c/p}(T, K; (\mu, \nu), N_q)$ for N_q quadrature points by substituting the integral in the equation with a finite sum⁶

$$V_{c/p}(T, K; (\mu, \nu), N_q) = \sum_{n=1}^{N_q} \lambda_n BS_{c/p}(t_0, S_0, T, K; \sigma_n). \quad (3.3)$$

The quadrature points σ_n and quadrature weights λ_n can be obtained by computing the moments $\mu_i = \mathbb{E}[\vartheta^i] = e^{i\mu + i^2\nu^2/2}$ for all $i \leq 2N$ and computing the matrices M, R and J as described in Appendix A. To obtain the implied volatility surface of the randomized parametrization, we can use a root-finding algorithm to find the implied volatility for each option price given by $V_{c/p}(T, K; (\mu, \nu), N_q)$, or we can derive the expansion terms from Equation (2.19) to obtain an analytical expression for the implied volatility surface $\hat{\sigma}(T, K; (\mu, \nu))$. We examine a slice of the randomized surface for two different sets of parameters. Figure 3 show the results for the expansions with different numbers of coefficients and the “exact” implied volatility obtained through a root-solving algorithm. In the experiment, we use $r = 2\%$, $T = 2$ and $N_q = 4$ quadrature points.

⁶Note that this is a similar result as Brigo and Mercurio [4], since the randomized price is a mixture of Black-Scholes prices.

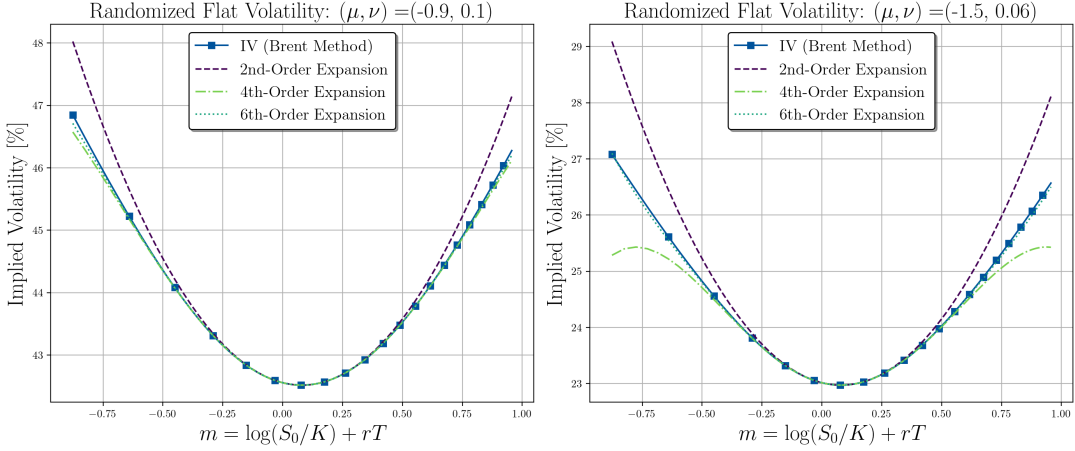


Figure 3: Randomized volatility slice for two different sets of parameters.

The randomization of the previously flat volatility surface yielded a new parametrization with two parameters μ, ν , which is able to form the characteristic ‘‘volatility smile’’. The result is a variant of the lognormal mixture model [4], which is known to be able to form a volatility smile. The main difference between the approaches is that the randomization defines the volatility smile using only two parameters, μ and η (excluding the choice of $N_q = 4$), offering a more parsimonious alternative to the lognormal mixture model, which uses seven parameters. While this may limit some flexibility compared to the discrete mixture model, it simplifies calibration and reduces computational complexity.

Figure 3 shows that the 6th-order approximation is able to closely match the exact implied volatility obtained from the root-finding algorithm. We observe that the fit is worse on the right-hand side for the lower-order expansions, although the shape of the implied volatility smile is similar. The reason is that the overall volatility level is lower on the right-hand side. This apparent increase in the importance of the higher-order coefficients can be explained by examining Equation (2.19), where each term is divided by a power of $a_0 = \frac{1}{2}\sigma(0)\sqrt{T}$. It should be reiterated, however, that there is no theoretical limit to the amount of expansion terms to be calculated.

The advantage of using the n -order expansion versus the application of a root-finding algorithm to the randomized pricing surface is based on the computation complexity. We examine the computational time for an increasing number of pairs (T, K) . The root finding algorithm uses Brent’s method and terminates once the relative difference between two estimates is at most $1e - 08$. If available, the method uses the implied volatility from the previous (usually neighboring) pair of (T, K) to increase the efficiency. Table 1 shows the comparison of the 2nd, 4th and 6th order approximation to the Brent’s method. The analytical method demonstrates a negligible increase in computation time as the number of strike/time pairs increases, due to its computational efficiency and independence from iterative procedures required by root-finding algorithms like Brent’s method.

Number of strike/time	10^3	10^4	$5.0 \cdot 10^4$	10^5
Brent (s)	0.102	1.1336	9.889	26.52
2nd-order expansion (s)	0.0009	0.001	0.001	0.001
4th-order expansion (s)	0.0006	0.0006	0.0007	0.0007
6th-order expansion (s)	0.0006	0.0007	0.0007	0.0008

Table 1: Comparison of analytic expansion vs Brent’s method for increasing amount of (T, K) : The analytical method is not affected by the increase in strikes, while the Brent method is expected to be $\mathcal{O}(n)$, although even slower in practice due to the increasing memory usage.

We conclude that the randomization of the flat volatility surface using a lognormal random variable allows us to create volatility smiles by adding a single parameter. Although the shape

of the smile can be altered by changing the parameter or even using an alternative distribution for ϑ , the additional flexibility is limited (see also [4] for a discussion on this issue).

3.2. Randomized SABR parametrization

In the second example, we consider the *SABR parametrization*, a well-known volatility parametrization introduced by Hagan et al. [15]. The parametrization is derived from the SABR model⁷ and given by the formula

$$\hat{\sigma}_H(T, K; (\alpha, \beta, \rho, \gamma)) = \frac{\alpha}{(F \cdot K)^{\frac{1-\beta}{2}} \left(1 + \frac{(1-\beta)^2}{24} \log^2 \left(\frac{F}{K} \right) + \frac{(1-\beta)^4}{1920} \log^4 \left(\frac{F}{K} \right) \right)} \cdot \left(\frac{z}{x(z)} \right) \\ \cdot \left(1 + \left(\frac{(1-\beta)^2}{24} \cdot \frac{\alpha^2}{(F \cdot K)^{1-\beta}} + \frac{1}{4} \cdot \frac{\rho \cdot \beta \cdot \gamma \cdot \alpha}{(F \cdot K)^{\frac{1-\beta}{2}}} + \frac{2-3\rho^2}{24} \cdot \gamma^2 \right) \cdot (T - t_0) \right), \quad (3.4)$$

where $F = e^{r(T-t_0)} S_0$ is the T -forward of the underlying and

$$z = \frac{\gamma}{\alpha} \cdot (F \cdot K)^{\frac{1-\beta}{2}} \cdot \log \left(\frac{F}{K} \right), \quad x(z) = \log \left(\frac{\sqrt{1-2\rho z+z^2}+z-\rho}{1-\rho} \right). \quad (3.5)$$

The SABR parametrization is defined by the set of 4 parameters $p = (\beta, \alpha, \rho, \gamma)$ on the parameter space

$$(\beta, \alpha, \rho, \gamma) \in \mathcal{D} = [0, 1] \times [0, \infty) \times (-1, 1) \times [0, \infty). \quad (3.6)$$

Although the parametrization defines an entire volatility surface, market practice is to use the SABR parametrization “slice-wise”, meaning that the calibration is done per volatility slice $\{K \mapsto \hat{\sigma}_{T_n}(K; \bar{p}), n \leq N\}$ for the set of N expiries observed in the market. The surface is then constructed by a linear interpolation, which is free of arbitrage under certain conditions. The details on the interpolation and the conditions are provided later.

Since the SABR parametrization is derived from a stochastic volatility model, the parametrization struggles to fit certain market scenarios in which the market does not follow the parametric regime, such as short-term index option chains. Almost perfect calibration is often impossible for these instances as the parameters reach their limits. We will use the methodology of parameter randomization on the SABR parametrization to increase its flexibility and show that with the help of randomization, the new parametrization will be able to fit the market better. In particular, the randomization substitutes the constant parameter γ with a Gamma random variable set by two parameters k, θ . The remaining parameters β, α, ρ are not randomized but remain deterministic, yielding a randomized parametrization of 5 parameters $\bar{p}^* = (\beta, \alpha, \rho, k, \theta)$. The parameters $k > 0, \theta > 0$ are the shape and scale parameter of a Gamma random variable $\vartheta \sim \Gamma(k, \theta)$ with probability density function

$$f_{\vartheta(k, \theta)}(x) = \frac{1}{\Gamma(k)\theta^k} x^{k-1} e^{-x/\theta}, \quad (3.7)$$

where $\Gamma(k)$ is the Gamma function. The random variable is almost surely positive, which makes it suitable for a randomization of γ , since the domain of γ is $[0, \infty)$. In this case, the randomized price function is given by

$$V_{c/p}(T, K; (\beta, \alpha, \rho, k, \theta)) = \int_0^\infty V_{c/p}(T, K; (\beta, \alpha, \rho, \gamma)) f_{\vartheta(k, \theta)}(\gamma) d\gamma. \quad (3.8)$$

⁷The SABR model is a stochastic volatility model with the same parameters, such that

$$dF_t = \sigma_t F_t^\beta dW_t, \\ d\sigma_t = \gamma \sigma_t dZ_t,$$

with $\sigma_0 = \alpha$ and the stochastic drivers such that $d\langle W_t, Z_t \rangle = \rho dt$.

We transform the continuous randomization into the discretized model. The moments of the Gamma distribution are given by $\mathbb{E}[\vartheta^i] = \theta^i \frac{\Gamma(k+i)}{\Gamma(k)}$ for any $0 \leq i \leq 2N_q$ and we obtain the randomized option price function as

$$V_{c/p}(T, K; (\beta, \alpha, \rho, k, \theta), N_q) = \sum_{n=1}^{N_q} \lambda_n V_{c/p}(T, K; (\beta, \alpha, \rho, \gamma_n)), \quad (3.9)$$

where $\{\lambda_n, \gamma_n\}_{n=1}^{N_q}$ are the quadrature weights and points of the Gamma distribution with parameters k, θ . The implied volatility $\hat{\sigma}(T, K, (\beta, \alpha, \rho, k, \theta), N_q)$ of the randomized SABR parametrization can be obtained by solving the inverse problem to obtain an exact solution, or by using the expansion of Theorem 2.4. Figure 4 shows the effect of the new parameters k, θ on the implied volatility shapes.

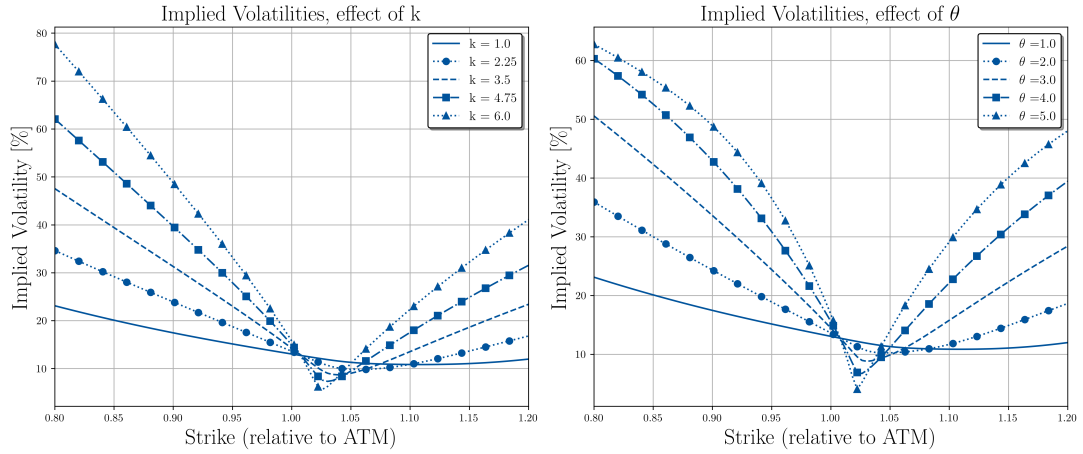


Figure 4: Implied volatility skew: The parameters k and θ have a strong effect on the shape of the implied volatility.

Although Figure 4 demonstrates how the new parameters influence the skew of the implied volatility curves, it remains unclear how the randomization of the γ parameter specifically enhances the fit of the traditional SABR parametrization. In the standard SABR parametrization, the γ parameter directly influences the skew of the implied volatility profile. After re-centering to the ATM volatility, a higher γ results in a more pronounced skew. It widens the difference between the maximum and minimum implied volatilities within a given strike range. Since γ is the sole parameter governing skew, control over the exact curvature of the skew is inherently limited.

By randomizing γ , we parameters that modulate not only the level of the skew, but also the curvature of the shape around the ATM point. To evaluate the impact of this modification, we conduct the following experiment: using the randomized SABR parametrization, we generate two sets of implied volatility quotes across 40 strikes. We then apply an optimizer to fit the traditional SABR parametrization to these quotes, resulting in nearly identical parameter values for both sets, specifically $(\beta, \alpha, \rho, \gamma) = (0.9, 0.25, -0.135, 3.5)$.

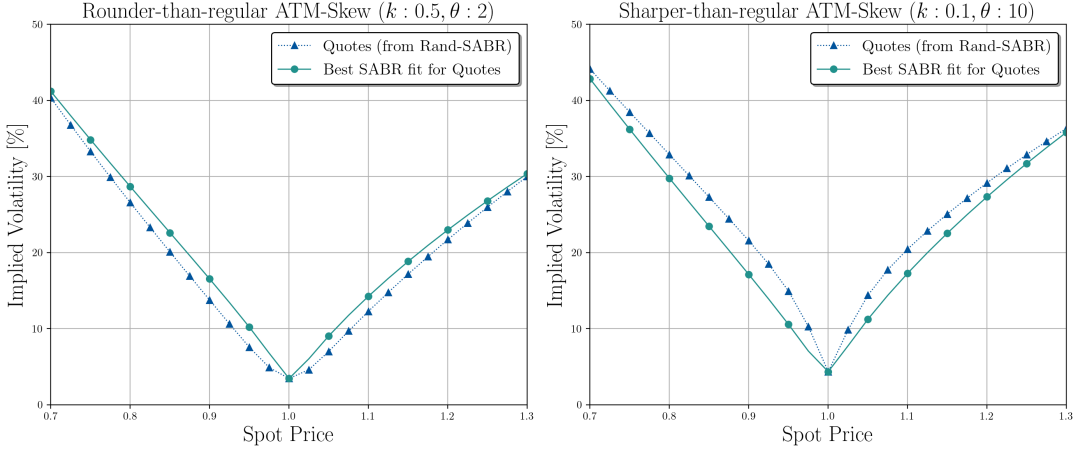


Figure 5: Comparison SABR vs Rand-SABR: The randomized parameters determine the curvature around the ATM point, while leaving the amount of the skew constant.

The experiment in Figure 5 shows that the SABR parametrization cannot account for the detailed curvature. The parametrization is limited by the choice of a single parameter. The randomization of the parameter helps to gain flexibility, which can be essential in fitting the market.

3.3. Fitting the model to the market

To study the flexibility of the new randomized SABR parametrization, we apply it to real data to examine its fit. We collect a set of short-maturity index options on the SPX index and obtain the market quotes for European put and call options on the 31st of July 2024 for a range of strikes and expiries. The data is downloaded from the Cboe data shop [5], which is based on actual transactions occurring on the Cboe exchange. Table 2 summarizes the data of the option chains and expiries available in the set. When both put and call quotes are available we select the most liquid quote per strike based on the open interest, which are the out-the-money quotes.

Expiry Date	Days to Maturity	N Quotes	Min Strike	Max Strike
Aug 16 2024	16	381	3175	6900
Sep 20 2024	51	356	3100	7200
Oct 18 2024	79	340	3100	9000
Nov 15 2024	107	289	3025	8600

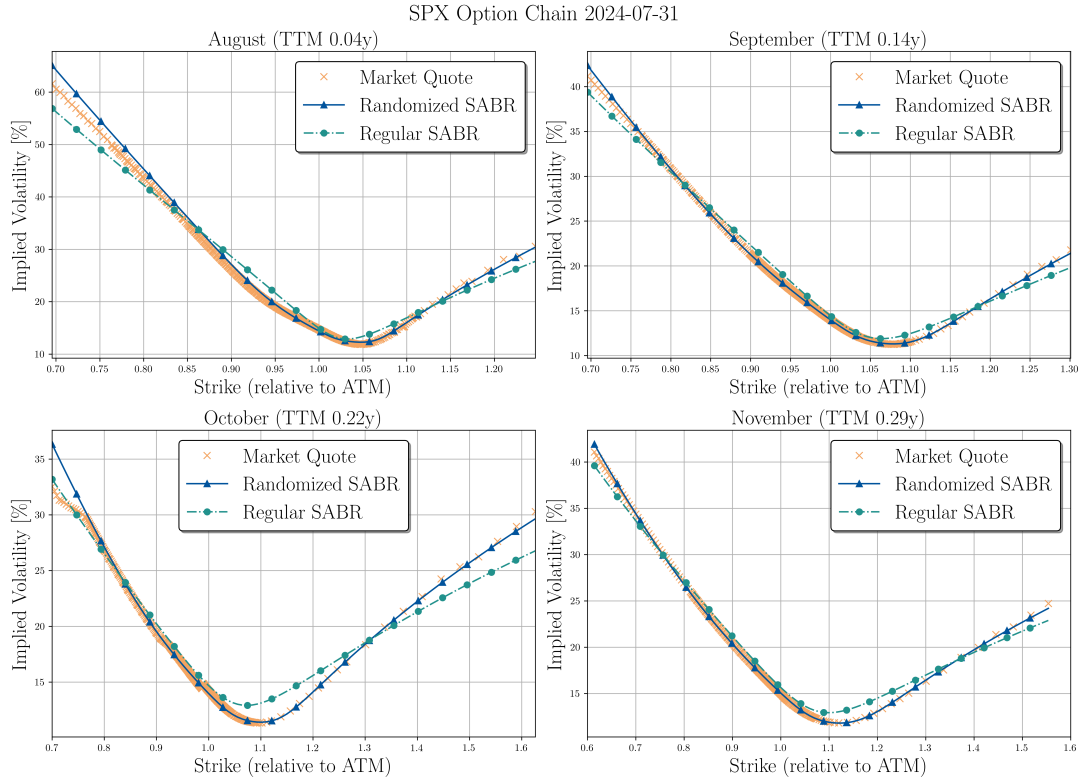
Table 2: Data summary implied volatilities quotes on Jul 31st, 2024

For the randomized SABR parametrization, we choose $N_q = 2$ quadrature points. Additionally, we fix $\beta = 0.9$ to reduce the number of parameters to calibrate, following common practice and empirical observations that this value provides a good balance between model flexibility and calibration stability [20]. The remaining parameters are fitted to the market quotes using an optimization scheme. The optimization can be achieved on the randomized prices given by Equation (3.9) or on the implied volatility surface using the expansion of Theorem 2.4. Table 3 shows the calibrated parameters for the randomized SABR parametrization.

Expiry	β	α	ρ	k	θ	Var Γ
Aug	0.9	0.335	-0.7	1.775	1.378	3.371
Sep	0.9	0.319	-0.681	3.872	0.455	0.802
Oct	0.9	0.318	-0.674	3.032	0.446	0.603
Nov	0.9	0.338	-0.687	4.916	0.271	0.361

Table 3: Parameter calibration Randomized SABR

To compare the fit, we also run the optimization on the regular SABR parametrization as a reference. The fit of the two models is shown in Figure 6 compared to the market quotes. We see that the randomized SABR parametrization has an excellent fit and can replicate the skew observed on the short-term maturity options on the SPX index.



	Sum Squared Errors (SSE)		Mean Squared Errors (MSE)	
Month	Regular SABR	Randomized SABR	Regular SABR	Randomized SABR
Aug	0.1248596	0.0414336	3.53E-04	1.17E-04
Sep	0.0192344	0.0009572	5.92E-05	2.90E-06
Oct	0.0233494	0.0113573	7.56E-05	3.68E-05
Nov	0.015732	0.0006516	5.74E-05	2.40E-06

Figure 6: Fit to the market: The randomized SABR parametrization has an excellent fit to the market data.

We observe from Table 3 that the variance of the randomized parameter ϑ , which is given by $\text{Var}(\vartheta) = k\theta^2$ decreases as the time to maturity increases. This shows that the longer the time-to-maturity, the less randomization is required to fit this observed market regime.

Since we fit the SABR parametrization slice-wise, it remains to show the construction of an arbitrage-free surface with the slices. As the slices are necessarily arbitrage-free, the construction must be free of calendar arbitrage, governed by Condition v) from Definition 2.1. The condition states that the pricing function must be non-decreasing in the time direction, meaning that an interpolation scheme in the time direction is sufficient for the construction. Suppose that we calibrate a set of slices $\{\hat{\sigma}_{T_i}(K; \bar{p}_i^*, N_q) : i \leq N\}$, which are arbitrage-free in strike direction, and suppose that there is no calendar-spread arbitrage in the market. This means that, if $T_i \leq T_j$, then

$$V(T_i, K; \bar{p}_i^*, N_q) \leq V(T_j, K; \bar{p}_j^*, N_q), \quad \forall K \in \Pi_K. \quad (3.10)$$

It is well-known [9] that the absence of calendar-spread arbitrage is equivalent to the condition

that the *total implied variance* is increasing, i.e.

$$\hat{\sigma}_{T_i}^2(K; \bar{p}_i^*, N_q) T_i \leq \hat{\sigma}_{T_j}^2(K; \bar{p}_j^*, N_q) T_j, \quad \forall K \in \Pi_K. \quad (3.11)$$

Under this condition, a linear interpolation in total implied variance suffices to obtain an arbitrage-free volatility surface from the slices. Let $a \in [0, 1]$ be such that $T = (1-a)T_i + aT_j$ and define

$$\hat{\sigma}(T, K; \bar{p}^*, N_q) = \frac{1}{\sqrt{T}} \sqrt{(1-a)\hat{\sigma}_{T_i}^2(K; \bar{p}_i^*, N_q) T_i + a\hat{\sigma}_{T_j}^2(K; \bar{p}_j^*, N_q) T_j}, \quad \forall K \in \Pi_K. \quad (3.12)$$

This shows that if the calibrated slices are consistent in time, meaning that Equation (3.10) is true, the linear interpolation and the calibrated slices define an arbitrage-free surface for all $T \in [T_1, T_N]$. This concludes the randomization of the SABR parametrization.

4. Randomized Spot Volatility Parametrizations & Near Expiry Options for Equities

In this section of this paper, we consider an extension of the randomization of parametric volatility surfaces to a randomization of the spot price S_0 , which follows the same principles as the regular randomization. The new randomization, which we refer to as the *spot randomization*, replaces the usually predetermined variable of the spot price S_0 with a random variable ϑ . We will show below that, under certain conditions, such a randomization of the spot price is arbitrage-free, and that this parametrization is particularly effective to model option markets of very short-term options, known as *near-expiry options*. Near expiry options, also known as *zero-day-expiry options* (ODTE) options⁸ are options whose maturity date is imminent, i.e., only a few days in the future, or even expire at the end of the day. On the day of an earning announcement, these options chains sometimes exhibit volatility slices with one or more concave sections, such as the W-shaped implied volatility slice or the “mustache”- shape [1, 10]. The unusual shape of implied volatility is an indication of a *bimodal* or *multimodal* risk-neutral probability distribution⁹, i.e. a probability distribution function which exhibits two modes. The rationale is that the uncertainty from the earnings yields a multi-modal risk-neutral probability distribution of S_T , reflecting the evolution of the stock price given different scenarios from the earnings (i.e., positive surprise vs negative surprise). Traditional implied volatility parametrizations, which have their origins in stochastic diffusion models, such as the SABR parametrization or the SVI, struggle to produce such shapes since the stochastic driver, which is a diffusion process, is inherently single-modal. The novel randomization method on the spot price offers a valuable solution in this case, as the randomization of the spot price offers an effective way to create superpositions of the PDFs with different (single) modes, yielding a mixture density of a similar kind to the lognormal mixture model as described in Glasserman and Pirjol [10]. We will prove that the randomized volatility shape is arbitrage-free and show that it produces excellent results on the empirical data, utilizing data from the ticker AMZN on the day of the earning announcement for Q1 in April 2018. Since the options we consider are short-expiry options, we will focus the fitting of the data on a single volatility slice for a fixed time T . Although the randomization still provides an entire implied volatility surface, the main purpose of the spot randomization is to fit the non-standard volatility shape and to provide a viable price for any strike for the given expiry.

4.1. Randomized Spot Prices

Suppose that $\hat{\sigma}(T, K, \bar{p})$ is a parametrization with parameters \bar{p} and let $p_{S_T; \bar{p}}$ be the risk-neutral PDF given by the parametrization for an asset S at the fixed time T . Since the risk-neutral probability density is a PDF of a random variable S_T , a necessary condition for it to be arbitrage-free is that S_T is centered at its forward $S_0 e^{r(T-t_0)}$. This can be shown as if

$$p_{S_T; \bar{p}}(x) = e^{r(T-t_0)} \frac{d^2 V_c(t_0, S_0, T, x; \bar{p})}{dx^2}, \quad (4.1)$$

⁸To be precise, ODTE options have a time-to-maturity of less than a day. Since we also consider options of 1-3 days expiry, we prefer the expression *near expiry options*.

⁹Although note that this is neither a sufficient nor a necessary condition.

then, an integration of Equation (4.1) multiplied with x shows that the expectation of S_T is $\mathbb{E}[S_T] = S_0 e^{r(T-t_0)}$. If we assume ϑ to be an absolutely continuous random variable with mean $\mathbb{E}[\vartheta] = S_0$ and assume it is almost surely positive, we can consider a randomization of the spot price by replacing S_0 with the random variable ϑ . As it will be presented later, the fact that it is centered at S_0 is necessary to ensure that the randomization is arbitrage-free. Denoting $f_\vartheta(x)$ the PDF of ϑ , we find equivalently to Equation (2.7):

$$\mathbb{E}[V_{c/p}(\vartheta, T, K; \bar{p})] = \int_{\mathbb{R}} BS_{c/p}(t_0, \theta, T, K; \hat{\sigma}(T, K; \bar{p})) f_\vartheta(\theta) d\theta, \quad (4.2)$$

where the value of the call/put options is now denoted by $V_{c/p}(S_0, T, K; \bar{p})$ with the extra parameter S_0 . The randomized price surface Equation (4.2) is an average of Black-Scholes prices, but the varying parameter is the spot price, as opposed to the parameters \bar{p} as before. Ensuring that the spot randomization is given in terms of a set of parameters, we define an extended parameter vector $\bar{p}^* = (p_1, p_2, \dots, p_m, q_1, q_2, \dots) \in \mathcal{D}^*$, which contains all previous parameters plus the parameters (q_1, q_2, \dots) specifying the distribution of ϑ . This defines the pricing surface of the spot randomization, and we can define the randomized volatility surface $\hat{\sigma}_s(T, K; \bar{p}^*)$ with the new parameter set as the Black-Scholes inverse of Equation (4.2).

Lemma 4.1 (Arbitrage-free spot randomization). *Let ϑ be centered at S_0 , absolutely continuous and almost surely positive. Then, the randomized spot volatility surface $\hat{\sigma}_s(T, K; \bar{p}^*)$, given by Equation (4.2), is arbitrage-free.*

Proof. We will show that we can write $\mathbb{E}[V_{c/p}(\vartheta, T, K; \bar{p})]$ as an integral of a proper probability density function centered at $S_0 e^{r(T-t_0)}$, which is sufficient to ensure the absence of arbitrage [4]. Suppose that $p_{S_T; \theta}$ is the PDF according to Equation (4.1), where S_0 is replaced with θ . In this case, we obtain

$$\begin{aligned} \mathbb{E}[V_{c/p}(\vartheta, T, K; \bar{p})] &= \int_{\mathbb{R}} BS_{c/p}(t_0, \theta, T, K; \hat{\sigma}_s(T, K; \bar{p})) f_\vartheta(\theta) d\theta \\ &= \int_{\mathbb{R}} \int_K^\infty (x - K) p_{S_T; \theta}(x) f_\vartheta(\theta) dx d\theta \\ &= \int_K^\infty (x - K) \int_{\mathbb{R}} p_{S_T; \theta}(x) f_\vartheta(\theta) d\theta dx \\ &= \int_K^\infty (x - K) \mathbb{E}[p_{S_T; \theta}(x)] dx. \end{aligned} \quad (4.3)$$

The expression $x \mapsto \mathbb{E}[p_{S_T; \theta}(x)]$ is a probability density function since it is a convex combination of proper PDFs. It remains to show that it is centered in $S_0 e^{r(T-t_0)}$, which is required for the absence of arbitrage.

$$\begin{aligned} \int_0^\infty x \mathbb{E}[p_{S_T; \theta}(x)] dx &= \int_0^\infty x \int_{\mathbb{R}} p_{S_T; \theta}(x) f_\vartheta(\theta) d\theta dx \\ &= \int_{\mathbb{R}} \int_0^\infty x p_{S_T; \theta}(x) dx f_\vartheta(\theta) d\theta \\ &= \int_{\mathbb{R}} \theta e^{r(T-t_0)} f_\vartheta(\theta) d\theta \\ &= \mathbb{E}[\vartheta] e^{r(T-t_0)} \\ &= S_0 e^{r(T-t_0)}. \end{aligned} \quad (4.4)$$

This concludes the proof. ■

It is apparent that as long as ϑ is centered at S_0 , the randomization does not induce any butterfly arbitrage, as the forward price, whose PDF is given by $\mathbb{E}[p_{S_T; \theta}(x)]$, is centered at $S_0 e^{r(T-t_0)}$. We will now continue the randomization process by discretizing the integral using the quadrature method. We define the discrete randomized pricing surface of the spot price as

$$V_{c/p}(T, K; \bar{p}^*, N_q) := \sum_{n=1}^{N_q} \lambda_n V_{c/p}(\theta_n, T, K; \bar{p}), \quad (4.5)$$

where $\{\lambda_n, \theta_n\}_{n \leq N_q}$ are the $N_q \in \mathbb{N}$ quadrature pairs of ϑ .

An interesting example of the spot randomization is the following:

Example 4.1. Suppose we obtain the risk-neutral probability density function $f_{S_T}(\cdot)$ of the asset price at a fixed expiry T . Consider a spot randomization of the parametric surface $\hat{\sigma}(T, K, \sigma) = \sigma$ with $\sigma = 0$ and random spot price given by the PDF of $f_{S_T}(\cdot)$. If $\hat{\sigma}(T, K, \sigma) = 0$, the call option price $V_c(S_0, T, K, \sigma)$ is given by $(S_0 - K)^+$, which means that

$$\mathbb{E}[V_c(\vartheta, T, K; 0)] = \int_{\mathbb{R}} V_c(\theta, T, K, \sigma) f_{S_T}(\theta) d\theta = \int_{\mathbb{R}} (\theta - K)^+ f_{S_T}(\theta) d\theta.$$

The right-hand side is exactly the call option price function given the risk-neutral probability density function $f_{S_T}(\cdot)$. The randomization therefore perfectly prices any option with expiry T .

The discretized spot randomization is given by (4.5). With the same technique of Theorem 2.4 we aim to derive the expansion of the implied volatility surface by setting up an implicit equation

$$f_{\text{spot}}(m, P_{(T,K)}(m)) = g_{\text{spot}}(m), \quad (4.6)$$

for Equation (4.5). While the definition of $f_{\text{spot}}(m, P_{(T,K)}(m)) = f(m, P_{(T,K)}(m))$ remains the same as in of Equation (2.16), we redefine the function $g(m)$ to incorporate the randomization of the spot instead of the volatility. Note that in the summation of the Black-Scholes formulae, the terms no longer depend on S_0 but on θ_n . Writing

$$\log(\theta_n/K) + rT = \log(S_0/K) + \log(\theta_n/S_0) + rT = m + \log(\theta_n/S_0), \quad (4.7)$$

we can define the new right-hand side of Equation (4.5) to obtain

$$g_{\text{spot}}(m) := S_0 \sum_{n=1}^{N_q} \lambda_n \left[\frac{\theta_n}{S_0} \Phi\left(\frac{m + \log(\frac{\theta_n}{S_0}) + \frac{1}{2}\eta^2 T}{\eta\sqrt{T}}\right) - e^{-m} \Phi\left(\frac{m + \log(\frac{\theta_n}{S_0}) - \frac{1}{2}\eta^2 T}{\eta\sqrt{T}}\right) \right], \quad (4.8)$$

where $\eta = \hat{\sigma}(T, K; \bar{p})$ is the implied volatility from the parametrization. The implicit function theorem then yields:

Theorem 4.2. The randomized spot implied volatility surface $\hat{\sigma}_s(T, K; \bar{p}^*)$ at $(T, K) \in \Pi$ is given by $P_{(T,K)}(m(T, K))$, for $m(T, K) = \log(S_0/K) + rT$, where the function $P_{(T,K)}$ has a Taylor expansion series

$$P_{(T,K)}(m) = P_{(T,K)}(0) + P'_{(T,K)}(0)m + \frac{P_{(T,K)}^{(2)}(0)}{2!}m^2 + \frac{P_{(T,K)}^{(3)}(0)}{3!}m^3 + \frac{P_{(T,K)}^{(4)}(0)}{4!}m^4 + \mathcal{O}(m^5), \quad (4.9)$$

with

$$\begin{aligned} P_{(T,K)}(0) &= \frac{2}{\sqrt{T}} \cdot \Phi^{-1} \left[\frac{1}{2} \left(1 + \sum_{n=1}^{N_q} \lambda_n \Sigma_n \right) \right], \\ P'_{(T,K)}(0) &= \left[\sum_{n=1}^{N_q} \lambda_n \left(\frac{\Sigma_n}{\eta\sqrt{T}} + \Phi(d_n^-) \right) - \Phi(d_0^-) \right] \cdot \frac{1}{\sqrt{T}\phi(d_0^-)}, \\ P_{(T,K)}^{(2)}(0) &= \left[\sum_{n=1}^{N_q} \lambda_n \left(\frac{\Sigma'_n + 2\phi(d_n^-)}{\eta\sqrt{T}} - \Phi(d_n^-) \right) - \Sigma'_0 \right] \cdot \frac{1}{\sqrt{T}\phi(d_0^-)}, \end{aligned}$$

and auxiliary variables

$$\begin{aligned} d_n^\pm &:= \frac{\log(\frac{\theta_n}{S_0}) \pm \frac{1}{2}\eta^2 T}{\eta\sqrt{T}}, \quad d_0^\pm := \pm \frac{1}{2}P_{(T,K)}(0)\sqrt{T}, \quad \Sigma_n := \frac{\theta_n}{S_0} \Phi(d_n^+) - \Phi(d_n^-), \\ \Sigma'_n &:= \frac{\theta_n}{S_0} \Phi(d_n^+) \left(\frac{\log(\theta_n/S_0)}{\eta^2 T} + 1/2 \right) - \Phi(d_n^-) \left(\frac{\log(\theta_n/S_0)}{\eta^2 T} - 1/2 \right), \\ \Sigma'_0 &:= -\Phi(d_0^-) + \phi(d_0^-) \left(\frac{1}{P_{(T,K)}(0)\sqrt{T}} + \sqrt{T}P'_{(T,K)}(0) - \frac{1}{4}P_{(T,K)}(0)(P'_{(T,K)}(0))^2 T^{3/2} \right). \end{aligned}$$

The terms for $P_{(T,K)}^{(3)}(0), P_{(T,K)}^{(4)}(0)$ are contained in [Appendix B](#).

Proof. The proof follows the same reasoning as Theorem [2.4](#), with the implicit equation given by Equation [\(4.6\)](#). \blacksquare

Remark (Odd-order terms no longer vanish). Note that contrary to Theorem [2.4](#), the odd-order derivatives do not vanish. This is caused by the fact that the arguments of $\Phi(\cdot)$ in $g_{\text{spot}}(m)$ are no longer symmetric due to the addition of $\log(\theta_n/S_0)$. This means that the amount of terms in the expansion grows very quickly.

We further note that the calculation of sensitivities, in particular the delta and gamma, is still feasible under the spot randomization. Since the surface $\hat{\sigma}_s(T, K; \bar{p}^*)$ is an analytic function of S_0 , the derivative $\frac{\partial \hat{\sigma}_s(T, K; \bar{p}^*)}{\partial S_0}$ can be simply derived analytically. In the case a finite difference approach is used, the shocking of the spot price by a quantity h will shift the random variable ϑ to $\vartheta + h$, which is then centered at $S_0 + h$.

4.2. Illustrative Example: Spot Randomization of Flat Surface

We will again first consider the simplest randomization, which is the flat volatility surface $\hat{\sigma}(T, K; \sigma) = \sigma$. Instead of replacing σ with a random variable, we randomize the spot price S_0 using a lognormal distributed random variable ϑ , such that $\log(\vartheta) \sim \mathcal{N}(\log(S_0) - \frac{\nu^2}{2}, \nu^2)$ given the parameter ν . The particular choice for the average ensures that

$$\mathbb{E}[\vartheta] = \exp\left(\log(S_0) - \frac{\nu^2}{2} + \frac{\nu^2}{2}\right) = S_0, \quad (4.10)$$

and therefore, that the randomization is arbitrage-free. We compute the prices, implied volatilities, and risk-neutral probability densities for various values of ν . The results are shown in Figure [7](#). The third graph shows that the risk-neutral probability density functions exhibits a bimodal shape, while the implied volatility is strongly concave. Next to the exact implied volatilities, we also plot 2nd to 4th-order approximations for the three shapes and highlight the convergence of the approximation to the exact implied volatility curve, which is derived using a root-finding scheme.

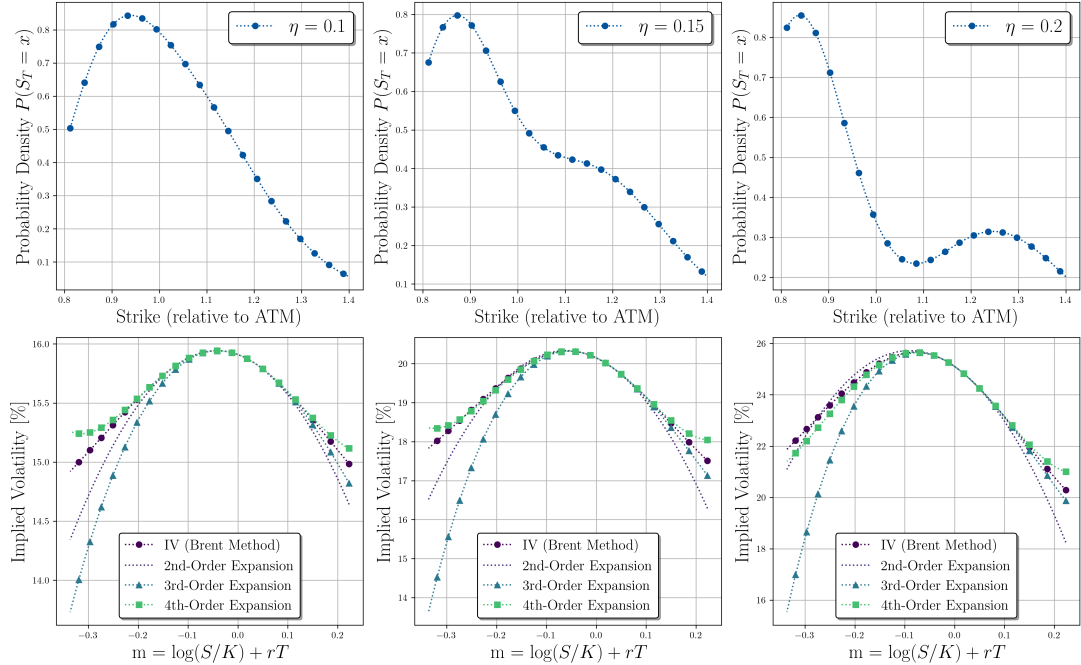


Figure 7: PDF and Implied Volatility of a randomized spot flat volatility surface. The implied volatility is derived from a root finder in the first few orders of approximations. The graph shows the convergence of the expansion to the reference graph.

We again examine the computational advantage of the analytical method compared to the “exact” method through a root-finding algorithm (Brent’s method). Since the root finder is repeated for every strike, the method is at least $\mathcal{O}(n)$. We run both the 4th order expansion and the root-finding algorithm for increasing numbers of strikes and compare the time used for calculation in Table 4.

Number of strikes	10^2	10^3	10^4
Brent (s)	0.23	2.36	26.61
4th-order expansion (s)	0.004	0.004	0.004

Table 4: Comparison of expansion vs. Brent’s method for increasing amount of strikes: The analytical method is not affected by the increase in strikes, while the Brent method is $\mathcal{O}(n)$.

4.3. Fitting an Earnings Announcement Volatility Surface

To demonstrate the capabilities of the randomization of the spot price, particularly in regard to earnings announcements, we consider an example of real market quotes. The company Amazon.com Inc. announced its earnings release for 2018 Q1 after market close on Apr 26th, 2018, which induced uncertainty in the market on the day of Apr 26th. We obtained the market quotes for options traded on the stock on the morning of the 26th (10:30 AM), which expire the next day on Apr 27th. Table 5 shows the summary statistics of the quotes which we obtain from the Cboe Data Shop [5].

Expiry Date	2018/04/27
Spot	1496.45
Min/Max Strike	1255/1607.5
N Quotes	126

Table 5: Summary Statistics AMZN options

Using the quotes, we fit a randomized spot SABR parametrization on the options quotes, where the spot price S_0 is again randomized with a log-normally distributed random variable ϑ , such that $\log \vartheta \sim \mathcal{N}(\log(S_0) - \frac{\nu^2}{2}, \nu^2)$. For the discretization, we choose $N_q = 2$ and run an optimization algorithm to obtain the optimal parameters for $\bar{p}^* = (\beta, \alpha, \rho, \gamma, \nu)$. As a benchmark, we also fit an SVI-type parametrization, which is not randomized, to the data. Figure 8 shows the fit of the implied volatility parametrizations, the market quotes, and the risk-neutral density from the randomized parametrization. The randomized spot parametrization is able to reproduce the shape of the implied volatility of the quotes. Furthermore, we see from the risk-neutral density this volatility shape stems from a bimodal probability density. The red line in the plot indicates the strike at the mean of the distribution (which is the forward-ATM). The SVI parametrization, on the other hand, fails to reproduce the implied volatility shape entirely, fitting to an essentially straight line.

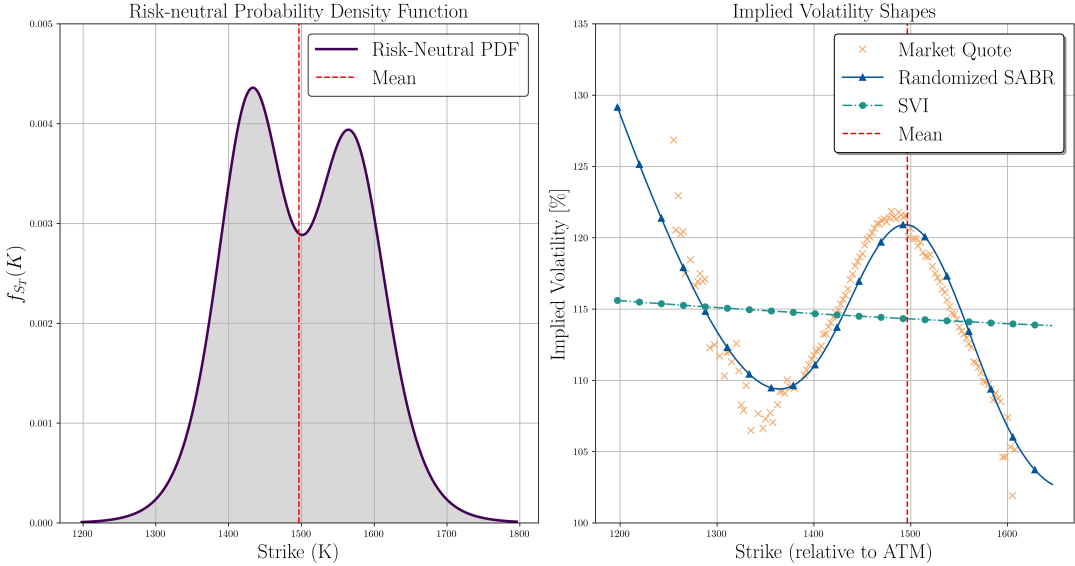


Figure 8: Risk-neutral PDF and implied volatilities of randomized parametrization.

5. Conclusion

The construction of a clean implied volatility surface is essential for accurately modeling financial derivatives, as it transforms discrete market option prices into a continuous, arbitrage-free representation. A well-defined volatility surface allows traders and risk managers to better understand the pricing dynamics of options across different strikes and maturities, facilitating more informed decision-making in the trading of derivatives. The traditional methods of constructing these surfaces often face challenges, particularly in capturing the nuances of market behavior, especially for options with shorter maturities.

This paper introduces a novel generic method to enhance the flexibility of volatility surface parametrizations through parameter randomization. We formulated new parametric surfaces from existing ones by replacing one of the parameters with a random variable. The method first defines a distribution for a set of parameters and then formulates the randomization as the expectation of the European option price under the distribution. This induces a mixture-type behavior in the pricing surface of the options and through Breeden-Litzenberger [3] also in the risk-neutral probability density functions. The mixture increases the flexibility of the price and, thus, provides a better ability to fit the market quotes when traditional parametrizations fail. Lastly, we derive an expansion of the implied volatility surface as a function of the input parameters, which can be computed to an arbitrary degree of accuracy. We presented two examples of randomized surfaces and showed that the randomized SABR parametrization is able to fit the data better than a classical SABR parametrization or an SVI-type parametrization.

In the second part of the paper, we utilized the randomization technique to formulate a randomized spot volatility surface. With this method, the spot price S_0 of the asset is randomized using a random variable centered at S_0 . This type of randomization is particularly effective in fitting volatility shapes that imply risk-neutral distribution functions of multi-modal form, which often occur shortly prior to earnings announcements of equities. Again, we derived an expansion of the implied volatility based on the same techniques as before and showed that the parametrization fits well with the data for near-maturity options during earnings announcements, a task that is impossible for classical diffusion-based parametrizations.

References

- [1] L. Alexiou, A. Goyal, A. Kostakis, and L. Rompolis. Pricing event risk: Evidence from concave implied volatility curves. *Swiss Finance Institute Research Paper*, pages 21–48, 2023.
- [2] J. Andreasen and B. Huge. Volatility interpolation. *Risk*, 24(3):76, 2011.

- [3] D. T. Breeden and R. H. Litzenberger. Prices of state-contingent claims implicit in option prices. *Journal of Business*, 51(4):621–651, 1978.
- [4] D. Brigo and F. Mercurio. Lognormal-mixture dynamics and calibration to market volatility smiles. *International Journal of Theoretical and Applied Finance*, 5(4):427–446, 2002.
- [5] Cboe. Cboe DataShop, 2024. URL <https://datashop.cboe.com/>.
- [6] J. Corbetta, P. Cohort, I. Laachir, and C. Martini. Robust calibration and arbitrage-free interpolation of SSVI slices. *Decisions in Economics and Finance*, 42(2):665–677, 2019.
- [7] M. R. Fengler. Arbitrage-free smoothing of the implied volatility surface. *Quantitative Finance*, 9(4):417–428, 2009.
- [8] J. Gatheral. *The volatility surface: A Practitioner’s Guide*. John Wiley and Sons, Inc, 2011.
- [9] J. Gatheral and A. Jacquier. Arbitrage-free SVI volatility surfaces. *Quantitative Finance*, 14(1):59–71, 2014.
- [10] P. Glasserman and D. Pirjol. W-shaped implied volatility curves and the Gaussian mixture model. *Quantitative Finance*, 23(4):557–577, 2023.
- [11] G. H. Golub and J. H. Welsch. Calculation of Gauss quadrature rules. *Mathematics of computation*, 23(106):221–230, 1969.
- [12] L. A. Grzelak. On randomization of affine diffusion processes with application to pricing of options on VIX and S&P 500. *arXiv:2208.12518*, 2022.
- [13] L. A. Grzelak, J. A. Witteveen, M. Suarez-Taboada, and C. W. Oosterlee. The stochastic collocation Monte Carlo sampler: highly efficient sampling from expensive distributions. *Quantitative Finance*, 19(2):339–356, 2019.
- [14] G. Guo, A. Jacquier, C. Martini, and L. Neufcourt. Generalized arbitrage-free svi volatility surfaces. *SIAM Journal on Financial Mathematics*, 7(1):619–641, 2016.
- [15] P. Hagan, D. Kumar, A. Leśniewski, and D. Woodward. Managing smile risk. *Wilmott Magazine*, pages 84–108, 2002.
- [16] C. Homescu. Implied volatility surface: Construction methodologies and characteristics. *arXiv preprint arXiv:1107.1834*, 2011.
- [17] S. G. Krantz and H. R. Parks. *The implicit function theorem: history, theory, and applications*. Springer Science & Business Media, 2002.
- [18] F. Le Floch. An arbitrage-free interpolation of class C2 for option prices. *Journal of Derivatives*, 28(4):64–86, 2021.
- [19] A. Mingone. No arbitrage global parametrization for the eSSVI volatility surface. *Quantitative Finance*, 22(12):2205–2217, 2022.
- [20] C. W. Oosterlee and L. A. Grzelak. *Mathematical Modeling and Computation in Finance: With exercises and Python and MATLAB computer codes*. World Scientific Publishing Europe Ltd, 2019.
- [21] M. P. V. Roper. *Implied volatility: General properties and asymptotics*. PhD thesis, UNSW Sydney, 2009.

Appendix A. Quadrature Pairs $\{\lambda_n, x_n\}_{n \leq N_q}$ for Expectations

Here, we present the derivation of the quadrature points to calculate the expectation of the randomized pricing surface. The section is based on [13] and Golub and Welsch [11], which establish the algorithm for the computation of the quadrature points for random variables based on the moments.

The Gaussian quadrature points enable an efficient approximation of the expectation $\mathbb{E}[g(X)]$ given an arbitrary function $g(\cdot)$ and an absolutely continuous random variable X , such that $f_X(x)$ is its probability density function. Since the expectation is an integral over the domain \mathcal{D} of X , the integral can be written as:

$$\mathbb{E}[g(X)] = \int_{\mathcal{D}} g(x) f_X(x) dx \approx \sum_{n=1}^{N_q} \lambda_n g(x_n), \quad (\text{A.1})$$

where $\{\lambda_n, x_n\}_{n \leq N_q}$ points are chosen in an optimal way, which we will establish below. The algorithm is general for any type of expectation and requires only an efficient computation of the moments $\mu_i = \mathbb{E}[X^i]$ of X . The foundation of the algorithm is to establish a sequence of polynomials $p_0(x), p_1(x), \dots$, which are orthonormal with respect to X , i.e., such that

$$\mathbb{E}[p_i(X)p_j(X)] = \begin{cases} 1 & \text{if } i = j, \\ 0 & \text{otherwise.} \end{cases} \quad (\text{A.2})$$

In this case, the quadrature points θ_n of degree N_q are given by the roots $p_{N_q}(\theta_n) = 0$ of $p_{N_q}(x)$, and the quadrature weights are given by a formula. Finding the quadrature pairs is thus reduced to obtaining a sequence of orthonormal polynomials. The polynomial sequence can be constructed from monomials $m_n(x) = x^n$, whose expectations are exactly equal to the moments μ_n of X . Denoting $\mu_{i,j} = \mu_{i+j} = \mathbb{E}[X^i X^j]$, the orthonormal polynomials can be

calculated the following way: first, we compute the $N_q + 1$ -dimensional Gram-matrix M given by

$$M = \begin{bmatrix} \mu_{0,0} & \mu_{0,1} & \cdots & \mu_{0,N_q} \\ \mu_{1,0} & \mu_{1,1} & \cdots & \mu_{1,N_q} \\ \vdots & \vdots & \ddots & \vdots \\ \mu_{N_q,0} & \mu_{N_q,1} & \cdots & \mu_{N_q,N_q} \end{bmatrix}, \quad (\text{A.3})$$

containing all moments until $2N_q$. Since the matrix is symmetric and positive semi-definite, we can use the Cholesky-decomposition $M = R^T R$ to obtain the triangular matrix R . Next, we calculate the quantities α_j and β_j , defined as

$$\alpha_j = \frac{r_{j,j+1}}{r_{j,j}} - \frac{r_{j-1,j}}{r_{j-1,j-1}}, \quad j = 1, \dots, N_q, \quad \text{and} \quad \beta_j = \left(\frac{r_{j+1,j+1}}{r_{j,j}} \right)^2, \quad j = 1, \dots, N_q - 1, \quad (\text{A.4})$$

where $r_{i,j}$ are the elements of the matrix R . Using the coefficients α, β , we can recursively define the polynomial sequence $p_n(x)$ as

$$p_{j+1} = (x - \alpha_j)p_j(x) - \beta_j p_{j-1}, \quad j = 1, \dots, N_q - 1, \quad (\text{A.5})$$

with $p_0 \equiv 0, p_1 \equiv 1$. One can show that the polynomials are indeed orthonormal and thus that the quadrature points are given by the roots of p_{N_q} . A bit of linear algebra shows that the roots can be found by the eigenvalues of the matrix

$$J := \begin{bmatrix} \alpha_1 & \sqrt{\beta_1} & 0 & 0 & \cdots & 0 \\ \sqrt{\beta_1} & \alpha_2 & \sqrt{\beta_2} & 0 & \cdots & 0 \\ \cdots & \cdots & \cdots & \cdots & \cdots & \cdots \\ 0 & \cdots & 0 & \sqrt{\beta_{N_q-2}} & \alpha_{N_q-1} & \sqrt{\beta_{N_q-1}} \\ 0 & \cdots & 0 & 0 & \sqrt{\beta_{N_q-1}} & \alpha_{N_q} \end{bmatrix}, \quad (\text{A.6})$$

and additionally the quadrature weights $\lambda_n = (v_1^n)^2$ by the square of the first row of the n -th eigenvalue v_n (see [11] for an extensive discussion). An implementation of the algorithm in Python and MATLAB can be found on [Github](#) [12].

Appendix B. Higher-Order (3rd,4th) Terms Calculation for Spot Randomization

Here, we present the 3rd and 4th order from the spot randomization of Theorem 4.2. We derived the terms by separately computing the partial derivatives $f_x = \frac{\partial f_{\text{spot}}}{\partial x} f_y = \frac{\partial f_{\text{spot}}}{\partial y}$ of f_{spot} , its higher order partial derivatives, and the derivative of the function $g_{\text{spot}}(m)$. Then, the expansion terms are given as

$$\begin{aligned} P^{(3)} &= \frac{1}{f_y} \left[g^{(3)} - f_{xxx} - 3f_{xxy}P' - 3f_{xyy}P'^2 - 3f_{xy}P^{(2)} - 3f_{yy}P'P^{(2)} - f_{yyy}P'^3 \right] \\ P^{(4)} &= \frac{1}{f_y} \left[g^{(4)} - f_{xxxx} - f_{yyyy}P'^4 - 4f_{xyyy}P'^3 - 4f_{yxxx}P' - 6f_{xxyy}P'^2 - 6f_{yyy}P'^2P^{(2)} - 12f_{xyy}P'P^{(2)} \right. \\ &\quad \left. - 6f_{xy}P^{(2)} - 4f_{yy}P^{(3)}P' - 6f_{yy}P^{(2)} - 4f_{xy}P^{(3)} \right], \end{aligned}$$

where we have used the short-hand notation

$$P = P_{(T,K)}(0), \quad P' = P'_{(T,K)}(0), \quad P^{(2)} = P^{(2)}_{(T,K)}(0), \quad P^{(3)} = P^{(3)}(0).$$

This yields the equations

$$\begin{aligned}
P^{(3)} &= \sum_{n=1}^{N_q} \left[\frac{1}{16T^2} \left(\frac{T (48P' + P (24 + PT (24P^{(2)} - 6PP'^2T + P'^3T (4 - P^2T) + 12P' (-1 + PP^{(2)}T))))}{P^2} \right. \right. \\
&\quad - \frac{24e^{\frac{1}{8}T(P-\eta)(P+\eta)-\frac{\beta_n^2}{2T\eta^2}} T \sqrt{e^{\beta_n}} \lambda_n}{\eta} \\
&\quad - 16e^{\frac{P^2T}{8}} \sqrt{2\pi} T^{3/2} \left(\Phi \left(\frac{P\sqrt{T}}{2} \right) - \lambda_n \Phi \left(\frac{T\eta^2 - 2\beta_n}{2\sqrt{T}\eta} \right) \right) \\
&\quad \left. \left. - \frac{16e^{\frac{1}{8}T(P-\eta)(P+\eta)-\frac{\beta_n^2}{2T\eta^2}} \sqrt{e^{\beta_n}} \lambda_n \beta_n}{\eta^3} \right) \right] \\
P^{(4)} &= \sum_{n=1}^{N_q} \left[\frac{\eta^2}{64P^3T^2\eta^5} \left(64 + T\eta^3 \left(-768P'^2 + 384P (-P' + P^{(2)}) \right. \right. \right. \\
&\quad + 8P^5P'^2 (P' - 3P^{(2)}) T^3 + P^6P'^4T^4 - 16P^2 (7 + 6P'^2T) \\
&\quad + 32P^3T (P' - 3P^{(2)} + 4P^{(3)} - P'^2 (P' - 3P^{(2)}) T) \\
&\quad + 4P^4T^2 (24P^{(2)} + P' (6P' - 24P^{(2)} + 16P^{(3)} - 3P'^3T)) \\
&\quad \left. \left. + 16e^{\frac{1}{8}T(P-\eta)(P+\eta)} P^3 (-4 + 7T\eta^2) \sqrt{e^{\beta_n}} \lambda_n \right) \right. \\
&\quad + 32\Sigma_n P^3 \left(\frac{e^{\frac{P^2T}{8}}}{\Sigma_n} \sqrt{2\pi} T^{5/2} \eta^5 \left(\Phi \left(\frac{P\sqrt{T}}{2} \right) - \lambda_n \Phi \left(\frac{T\eta^2 - 2\beta_n}{2\sqrt{T}\eta} \right) \right) \right. \\
&\quad + 4\Sigma_n e^{\frac{1}{8}T(P-\eta)(P+\eta)} T\eta^2 \sqrt{e^{\beta_n}} \lambda_n \beta_n \\
&\quad \left. \left. + 2e^{\frac{1}{8}T(P-\eta)(P+\eta)} \sqrt{e^{\beta_n}} \lambda_n \beta_n^2 \right) \right],
\end{aligned}$$

with

$$\beta_n = \log(\theta_n/S_0) \quad \text{and} \quad \Sigma_n = e^{-\frac{\beta_n^2}{2T\eta^2}}.$$